

## Structure-Based Optimization of Novel Azepane Derivatives as PKB Inhibitors

Christine B. Breitenlechner,<sup>‡</sup> Thomas Wegge,<sup>†</sup> Laurent Berillon,<sup>†</sup> Klaus Graul,<sup>†</sup> Klaus Marzenell,<sup>†</sup> Walter-Gunar Friebe,<sup>†</sup> Ulrike Thomas,<sup>†</sup> Ralf Schumacher,<sup>†</sup> Robert Huber,<sup>‡</sup> Richard A. Engh,<sup>†,‡</sup> and Birgit Masjost<sup>\*,†</sup>

Pharma Research, Roche Diagnostics GmbH, Werk Penzberg, Nonnenwald 2, D-82372 Penzberg, Germany, and Abteilung für Strukturforschung, MPI für Biochemie, Am Klopferspitz 18a, D-82152 Martinsried, Germany

Received October 1, 2003

Novel azepane derivatives were prepared and evaluated for protein kinase B (PKB- $\alpha$ ) and protein kinase A (PKA) inhibition. The original (–)-balanol-derived lead structure (4*R*)-4-(2-fluoro-6-hydroxy-3-methoxy-benzoyl)-benzoic acid (3*R*)-3-[(pyridine-4-carbonyl)amino]-azepan-4-yl ester (**1**) (IC<sub>50</sub> (PKB- $\alpha$ ) = 5 nM) which contains an ester moiety was found to be plasma unstable and therefore unsuitable as a drug. Based upon molecular modeling studies using the crystal structure of the complex between PKA and **1**, the five compounds *N*-{(3*R*,4*R*)-4-[4-(2-fluoro-6-hydroxy-3-methoxy-benzoyl)-benzoylamino]-azepan-3-yl}-isonicotinamide (**4**), (3*R*,4*R*)-*N*-{4-[4-(2-fluoro-6-hydroxy-3-methoxy-benzoyl)-benzyloxy]-azepan-3-yl}-isonicotinamide (**5**), *N*-{(3*R*,4*S*)-4-[4-(2-fluoro-6-hydroxy-3-methoxy-benzoyl)-phenylamino]-methyl}-azepan-3-yl)-isonicotinamide (**6**), *N*-{(3*R*,4*R*)-4-[4-(2-fluoro-6-hydroxy-3-methoxy-benzoyl)-benzylamino]-azepan-3-yl}-isonicotinamide (**7**), and *N*-{(3*R*,4*S*)-4-[4-(*trans*-2-[4-(2-fluoro-6-hydroxy-3-methoxy-benzoyl)-phenyl]-vinyl)-azepan-3-yl]-isonicotinamide (**8**) with linkers isosteric to the ester were designed, synthesized, and tested for in vitro inhibitory activity against PKA and PKB- $\alpha$  and for plasma stability in mouse plasma.<sup>1</sup> Compound **4** was found to be plasma stable and highly active (IC<sub>50</sub> (PKB- $\alpha$ ) = 4 nM). Cocrystals with PKA were obtained for **4**, **5**, and **8** and analyzed for binding interactions and conformational changes in the ligands and protein in order to rationalize the different activities of the molecules.

### Introduction

Cell signaling pathways regulate cell growth, proliferation, and apoptosis. Kinases are the key players in cell signaling. They transduce signals from growth factor receptors for cell growth or apoptosis by phosphorylation of their substrates which are mostly downstream kinases involved in cell signaling processes themselves. The activity of kinases is regulated by phosphorylation and dephosphorylation effecting conformational changes in the kinases. Overexpression or constitutive activation of kinases involved in anti-apoptotic or proliferation signaling pathways are one typical feature of tumor cells.<sup>2</sup>

PKB is located downstream in the PI-3 kinase pathway<sup>3,4</sup> and phosphorylates a growing list of substrates involved in several pathways for cell survival and inhibition of apoptosis as has been shown recently.<sup>5–9</sup> Constitutive activation of PKB- $\alpha$  is frequently found in human prostate,<sup>10,11</sup> breast,<sup>12</sup> and ovarian carcinomas. It is due to a complete loss of the lipid phosphatase PTEN gene, a negative regulator of the PI-3 kinase pathway.<sup>13</sup> These data indicate that PKB- $\alpha$  is a central player in tumorigenesis and a potential target for cancer intervention.<sup>14</sup> Inhibitors of PKB- $\alpha$  are therefore promising drugs for cancer therapy as effective sensitizers or inducers of apoptosis.<sup>15</sup>

PKB- $\alpha$  belongs to the AGC-family of serine/threonine protein kinases. There are three isoforms known

(PKB- $\alpha$ , PKB- $\beta$ , and PKB- $\gamma$ ). The kinase domain of PKB- $\alpha$  has a sequence homology identity with PKB- $\beta$  of 91% and with PKB- $\gamma$  of 88%. PKB- $\alpha$  also exhibits a sequence homology identity to PKC- $\eta$  of 53% and PKA-C $\alpha$  of 47%.<sup>16</sup> Recently, a crystal structure of PKB- $\beta$  with GSK3-peptide and AMP–PNP has been reported.<sup>17,18</sup> Several structural classes of PKC and PKA inhibitors are known. One class of PKC inhibitors with pharmaceutical potential are bisindolylmaleimides, derived from the natural product staurosporin.<sup>19–22</sup> Another important class of inhibitors is derived from the natural product (–)-balanol which was first isolated as a metabolite of the fungus *Verticillium balanoides* at Sphinx Pharmaceuticals (Eli Lilly) in 1993<sup>23</sup> and from a species of *Fusarium* at Nippon Roche in 1994.<sup>24</sup> (–)-Balanol inhibits PKC in the low nanomolar range. Cocrystallization of (–)-balanol with PKA was achieved in 1999.<sup>25,26</sup> Balanol derivatives with PKC inhibitory activity have been reported in the literature.<sup>27–35</sup>

In sum, these research results show PKB- $\alpha$  to be an attractive target in oncology. We found that certain novel azepane derivatives such as **1** are potent inhibitors of PKB- $\alpha$  in vitro and in various tumor cell lines (see Table 2). They also possess anti-cell-proliferation properties, and induce apoptosis. For the use as potential drugs with an in vivo effect on solid tumors, the compounds need to be stable in blood plasma. However, first in vitro experiments indicated that these compounds were not stable in mouse plasma. For compound **1** we measured a half-life time  $t_{1/2} < 1$  min. Therefore, the first optimization step to render these molecules potential drugs was to improve plasma stability. The

\* To whom correspondence should be addressed. Phone: +49(0)-8856/60 4749. Fax +49(0)8856/60-4445. E-mail: birgit.masjost@roche.com.

<sup>†</sup> Roche Diagnostics GmbH, Penzberg.

<sup>‡</sup> Max-Planck-Institut, Martinsried.

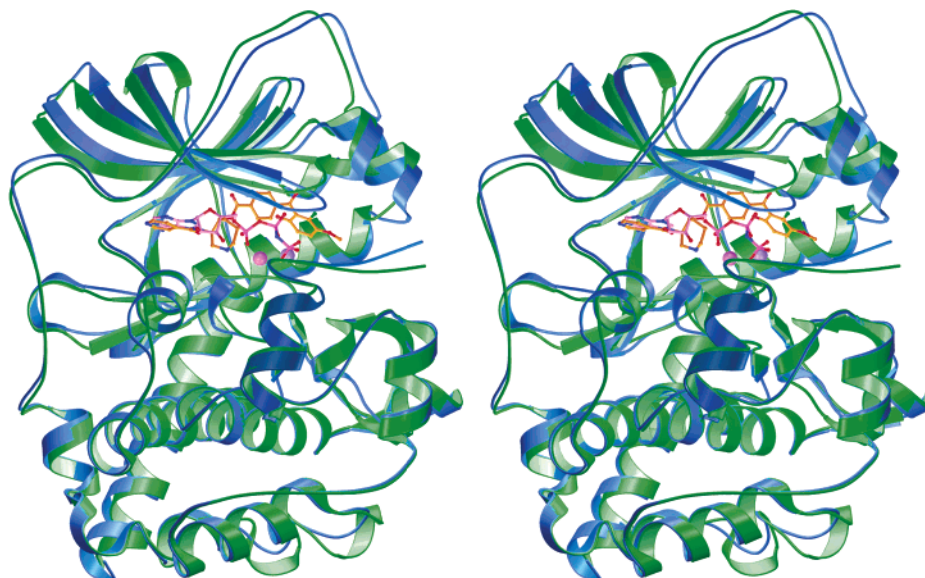


**Figure 1.** Overlay of X-ray crystal structures of inhibitor **1** (orange/green) and AMP-PNP and two Mn<sup>2+</sup> (magenta/blue) in complex with PKA and PKI(5–24). The backbone of the kinase domain of PKA is shown in  $\alpha$ -helix and  $\beta$ -sheet ribbon presentation.

instability is presumably caused by a rapid cleavage of the ester bond by ester hydrolases; LC-MS results show that cleavage products **2** and **3** appear after incubation of **1** at 37 °C in mouse plasma (Table 1). Therefore, we set out to find a replacement of the ester group which would not adversely affect the inhibitory activities of the molecules.

Because it crystallizes readily, PKA has been used as a surrogate kinase to study structural features of closely related enzymes such as Rho-kinase.<sup>36</sup> For similar reasons, we used PKA for cocrystallization with PKB- $\alpha$  inhibitors for rapid access to structural information on inhibitor binding, enabling structure-based guidance of inhibitor design issues.

Cocrystallization of **1** with PKA revealed the intermolecular bonding contacts between the amino acids of the enzyme and compound **1** as well as its binding conformation. Here we describe the rational design,<sup>37–40</sup> synthesis, and *in vitro* inhibitory activities of analogues of compound **1** with plasma stable linkers replacing the ester moiety.<sup>1</sup> These new inhibitors were also cocrystallized with PKA, and the X-ray structures are thoroughly analyzed for binding contacts and conformation of bound ligands to the enzyme.

## Results and Discussion

**Design and Prediction.** We cocrystallized compound **1** with PKA and PKI(5–24) in a ternary complex and solved the X-ray structure at 2.5 Å resolution under equal conditions as with AMP-PNP and other inhibitors before.<sup>25,41–44</sup> Figure 1 shows the overall structure of this complex superimposed with the AMP-PNP complex.<sup>41</sup> PKA consists of an N-terminal lobe and a C-terminal lobe. The ATP-binding site which the inhibitor molecules occupy is located inbetween these two lobes.

Figures 2a,b show the intermolecular bonding contacts in the complex between PKA and compound **1**. Three binding pockets were defined: the first contains the pyridine moiety and the amide connecting it to the azepane ring and will be referred to as pyridine pocket.

This space is occupied by the adenine in the complex of AMP-PNP and PKA<sup>41</sup> as shown in Figure 2b. Both aromatic systems are in the same plane. One of the amino acids involved in bonding interactions with these moieties is Val123 which makes an OCNH $\cdots$ N hydrogen bond to the pyridine via its main chain amide. This H-bond to Val123 or homologue is nearly universal among protein kinase inhibitor complexes and is apparently critical for tight binding inhibitors.<sup>36</sup> Furthermore, the amide makes hydrogen bonds with two water molecules, one of which is an OCNH $\cdots$ OH<sub>2</sub> H-bond to a water molecule that in turn hydrogen-bonds to the side chain carboxylate of Glu127 and to the carbonyl of the amide of Leu49; the other one is a HNCO $\cdots$ HO H-bond to a water molecule that is further hydrogen-bonded to the side chain amine of Lys72 and the side chain carboxylate of Asp184. Leu49, Val57, Ala70, Met120, Tyr122, Val123, Glu127, Leu173, Thr183, and Phe327 are involved in van der Waals contacts to the pyridine and amide portion of compound **1**. The second pocket, stretching over the ribose subsite, contains the azepane and the ester part of the molecule and will be referred to as the azepane pocket. It consists of three amino acids making hydrogen bonds to the NH<sub>2</sub><sup>+</sup> of the azepane ring: namely, Glu170 which makes a NHCO $\cdots$ HN hydrogen bond with its main chain CO to the NH<sub>2</sub><sup>+</sup> of the azepane ring, Asn171 which makes a hydrogen bond with its side chain CO to the NH<sub>2</sub><sup>+</sup> of the azepane ring, and Asp184 which makes a bifurcated hydrogen bond with its side chain COO to the NH<sub>2</sub><sup>+</sup> of the azepane ring. Moreover, Asp184 makes a COO $\cdots$ HO H-bond to the side chain of Thr183 and a COO $\cdots$ HO H-bond to a water molecule. Furthermore, Gly50, Thr51, Gly52, Val57, Lys72, Glu170, Asn171, and Asp184 make van der Waals contacts to the azepane and ester moiety. The third binding pocket contains the benzophenone part of the ligand and it will be called the benzophenone pocket. This pocket is covered by the flexible so-called glycine loop which is displaced compared to the AMP-PNP PKA complex (see Figure 1). Phe54 from the tip of the glycine loop has an OCNH $\cdots$ OC H-bond via its main

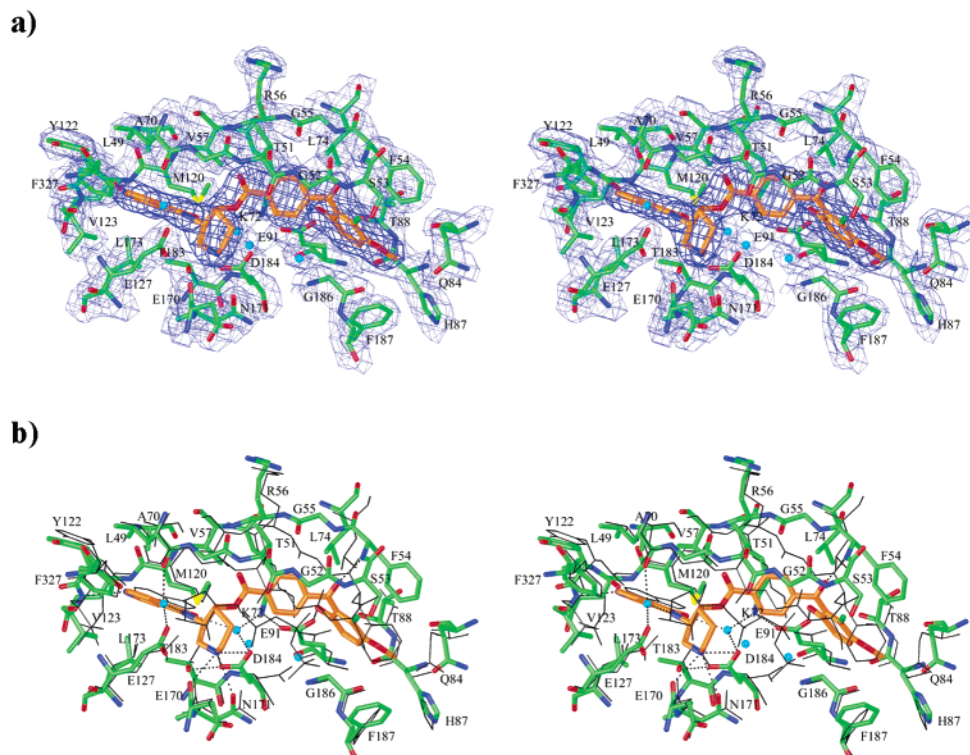


**Figure 2.** (a) X-ray crystal structure of inhibitor **1** situated in the active site of PKA with the final  $2F_o - F_c$  electron density map contoured at  $1\sigma$ . (b) Overlay of X-ray crystal structures of inhibitor **1** and AMP-PNP situated in the active site of PKA. The hydrogen bonds between the inhibitor **1** and the amino acids of PKA and water molecules are indicated.

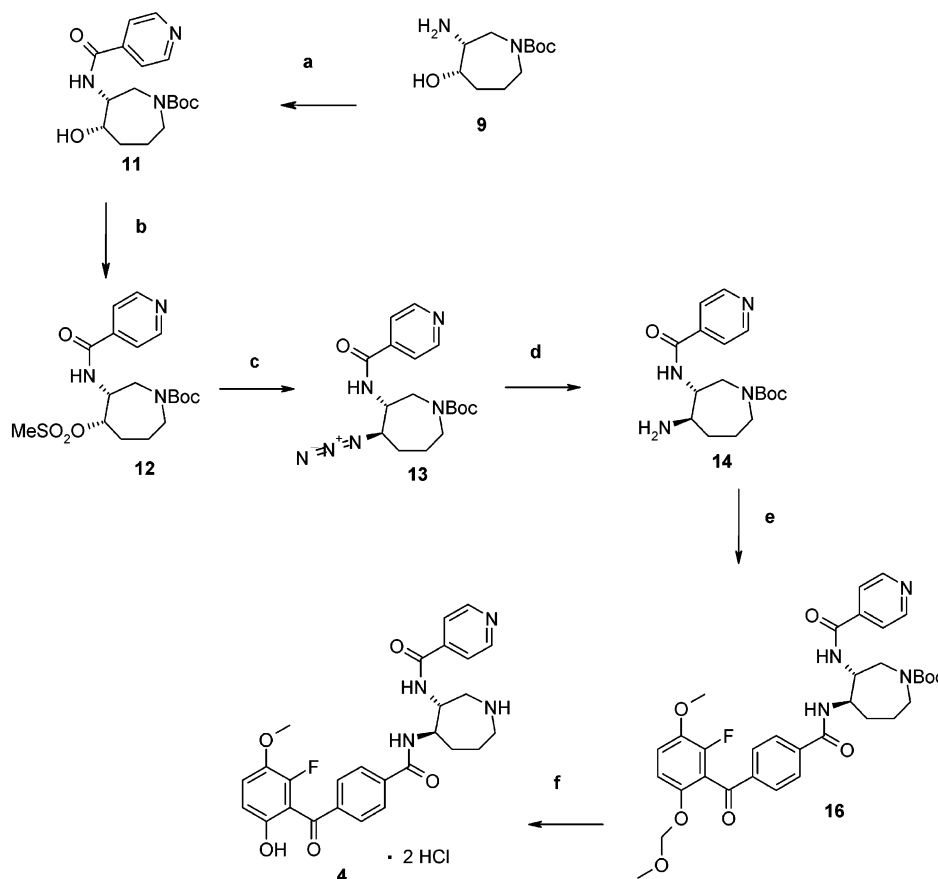
chain amide to the carbonyl oxygen of the benzophenone. Glu91 which is essential for catalysis<sup>45</sup> forms a salt bridge to the  $\text{NH}_3^+$  of Lys72 with its side chain COO in the active state as well as in the inhibitor complex with **1**. In this complex Glu91 also forms a  $\text{COO}\cdots\text{HO}$  hydrogen bond with its side chain to the inhibitor hydroxyl group of the benzophenone. In addition, Ser53, Phe54, Gly55, Arg56, Leu74, Gln84, His87, Thr88, Glu91, Gly186, and Phe187 make van der Waals contacts with the benzophenone moiety. The crystal structure shows that the plasma unstable ester moiety of compound **1** is not hydrogen-bonded to the enzyme. Also there are no strong attractive van der Waals interactions with the amino acids of PKA which are likely to make a significant contribution to the enthalpy of binding. On the other hand, its trans conformation rigidly orients the azepane and the benzophenone of **1** toward their binding pockets. We therefore sought to replace the ester moiety by an isosteric chemical linker to achieve plasma stability without losing potent inhibition. The design and estimation of relative binding affinities for the inhibitors **4**, **5**, **6**, **7**, and **8** was performed by computational methods, using the programs MOLOC<sup>46</sup> and Insight II.<sup>47</sup> Molecular modeling predicted that the double amide **4** and the compound with the vinyl linker **8** should have the highest binding affinities, mostly because these molecules have linkers that are preorganized in the trans conformation favored for binding (see Figure 2a). The inhibitors with the ether linkage **5** and the benzylamino linker **7** would have to rearrange to adopt the right conformation for binding which costs free energy. For the molecule with the phenylaminomethyl linker **6** we expected a significantly lower binding energy, because the molecule cannot adopt the conformation preferred for binding due to

steric hindrance between the methylene protons and the protons of the neighboring azepane ring.

**Synthesis.** For the synthesis of the various enantiopure balanol analogues (structurally related to (-)-balanol) such as **4**, **5**, **6**, **7**, and **8**, in which the carboxylic ester of the lead is replaced by different linkers, we employed five different synthetic routes. The synthesis of the double amide **4** started with *cis*-amino alcohol (**9**)<sup>48</sup> as chiral building block (Scheme 1). Treatment of starting material **9** with isonicotinic acid **10**/DCC/DMAP in methylene chloride yielded the isonicotinic amide **11**, which was transformed to the corresponding mesylate **12**.  $\text{S}_\text{N}2$ -type reaction of **12** by treatment with sodium azide afforded the *trans*-azide **13** which was selectively hydrogenated to the *trans* amine **14**. The second amide moiety was introduced by reacting amine **14** with acid **15**<sup>35</sup> in methylene chloride using DCC/DMAP as coupling reagents. Removal of the protecting groups from carbamate **16** led to the desired target compound **4** which could be isolated in 94% yield.

For the synthesis of the aniline **6**, a  $\text{S}_\text{N}2$ -type reaction of **12** with sodium cyanide yielded the *trans* cyanide **17**, which could not be isolated from elimination byproducts (Scheme 2). Hydrogenation of the raw material generated the unstable amine **18**. The key step in this synthetic pathway was the palladium-catalyzed Buchwald<sup>49</sup> coupling of aryl iodide **19** (synthesized from lithiated **20** and **21** as reaction partner and subsequent oxidation of the resulting carbinol **22**) with amine **18**. The desired coupling product **23** was deprotected using HCl in dioxane.

The synthesis of ether **5** was performed by protection of carbinol **24**<sup>35</sup> using TIPS-Cl (Scheme 3). Reduction with  $\text{LiAlH}_4$  yielded the hydroxymethyl compound **26** which could be transformed to the corresponding chlo-

Scheme 1<sup>a</sup>

<sup>a</sup> Reagents and conditions: (a) isonicotinic acid **10**, DCC, DMAP, CH<sub>2</sub>Cl<sub>2</sub>, r. t., 24 h, 98%; (b) MeSO<sub>2</sub>Cl, pyridine, rt, 24 h, 79%; (c) NaN<sub>3</sub>, DMF, 90 °C, 3 h, 91%; (d) Ra-Ni, 1 bar H<sub>2</sub>, CH<sub>3</sub>OH, 95%; (e) 4-(2-fluoro-3-methoxy-6-methoxymethoxy-benzoyl)-benzoic acid **15**,<sup>35</sup> DMAP, DCC, CH<sub>2</sub>Cl<sub>2</sub>, rt, 6 h, 76%; (f) 4 M HCl in dioxane, rt, 15 h, 94%.

romethyl compound **27** by treatment with PPh<sub>3</sub>/CCl<sub>4</sub>.<sup>50</sup> The ether was introduced by reacting chloromethyl compound **27** with amino alcohol **9**<sup>35,48</sup> and NaH to give **28**. Reaction of compound **28** with isonicotinic acid/DCC/DMAP in methylene chloride led to isonicotinic amide **29**. The carbinol function of the resulting ether **29** was selectively deprotected with TBAF and oxidized to the corresponding benzophenone **30** using activated MnO<sub>2</sub>. Deprotection with HCl in dioxane afforded the desired ether **5** in good yield.

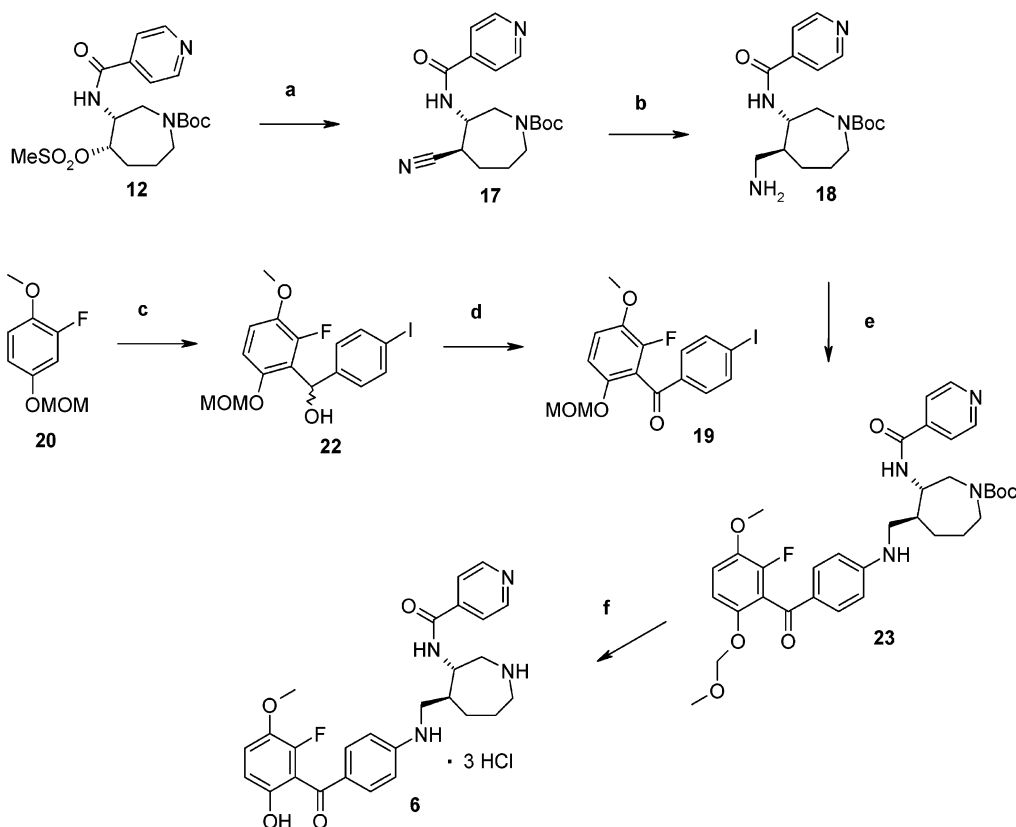
The synthetic pathway for benzylamine **7** was as follows: carbinol **24**<sup>35</sup> was converted to aldehyde **32** in two steps. Reduction (LiAlH<sub>4</sub>) of **24** afforded alcohol **31** and was followed by oxidation (activated MnO<sub>2</sub>) to give aldehyde **32** (Scheme 4). Reductive amination (NaCNBH<sub>3</sub>) of aldehyde **32** with amine **14** resulted in amine **34**. Subsequent deprotection with HCl in dioxane led to the desired balanol analogue **7**.

For the preparation of compound **8** with the *trans*-vinyl linker Swern oxidation<sup>51</sup> of **11** to ketone **35** and subsequent Wittig reaction (Ph<sub>3</sub>P<sup>+</sup>CH<sub>2</sub>OCH<sub>3</sub>Cl<sup>-</sup>, KO<sup>t</sup>Bu, ether) afforded enol ether **36** as an aldehyde synthon (Scheme 5). The enol ether **36** in CHCl<sub>3</sub> was thermodynamically hydrolyzed using Cl<sub>3</sub>CCOOH without deprotection of the carbamate group to the resulting aldehyde **37** which was a diastereomeric mixture (*trans*:*cis* = 3:1). The desired *trans*-aldehyde **37a** could not be separated from the *cis*-aldehyde **37b**. Therefore the diastereomeric mixture of aldehyde **37** was transformed

to vinyl compound **38** by Wittig reaction (Ph<sub>3</sub>P<sup>+</sup>CH<sub>3</sub>I<sup>-</sup>, *n*-BuLi, THF). At this stage the desired *trans*-vinyl compound could be isolated by preparative HPLC with chiral column OD 40 and 2-propanol/heptane = 1:4 as eluent. The aryl iodide **19** was coupled with the vinyl compound **38** using a Heck protocol<sup>52</sup> ((*o*-Tol)<sub>3</sub>P, Et<sub>3</sub>N, Pd(OAc)<sub>2</sub>, DMF) to yield the *trans*-vinyl compound **39**. Removal of the protecting groups with 2 N HCl in ether afforded the desired product **8**.

**Biological Results.** The plasma stability was determined for the inhibitors **1**, **4**, **5**, and **7**. Table 1 lists the half-lives of the molecules in mice blood plasma under the conditions mentioned above. All molecules except for the ester are plasma stable with half-lives *t*<sub>1/2</sub> > 29 h (compound **5**) up to 161 h (compound **7**). These findings confirm our hypothesis that the plasma instability of lead compound **1** is caused by cleavage of the ester bond. The biological activities of the compounds in the *in vitro* kinase assay are listed in Table 2. The most active compound is the double amide **4** (IC<sub>50</sub>(PKB-α) = 4 nM) as was predicted by molecular modeling, because the conformation of the amide is *trans*, and that is the preferred conformation of the linker in the bound state according to the crystal structure of **1** in PKA. The compound with the *trans*-vinyl linker **8** is considerably less active (IC<sub>50</sub>(PKB-α) = 160 nM) than the ester which was not predicted from the modeling.

The ether **5** (IC<sub>50</sub>(PKB-α) = 355 nM) is less active than double amide **4**, as predicted by modeling, presu-

Scheme 2<sup>a</sup>

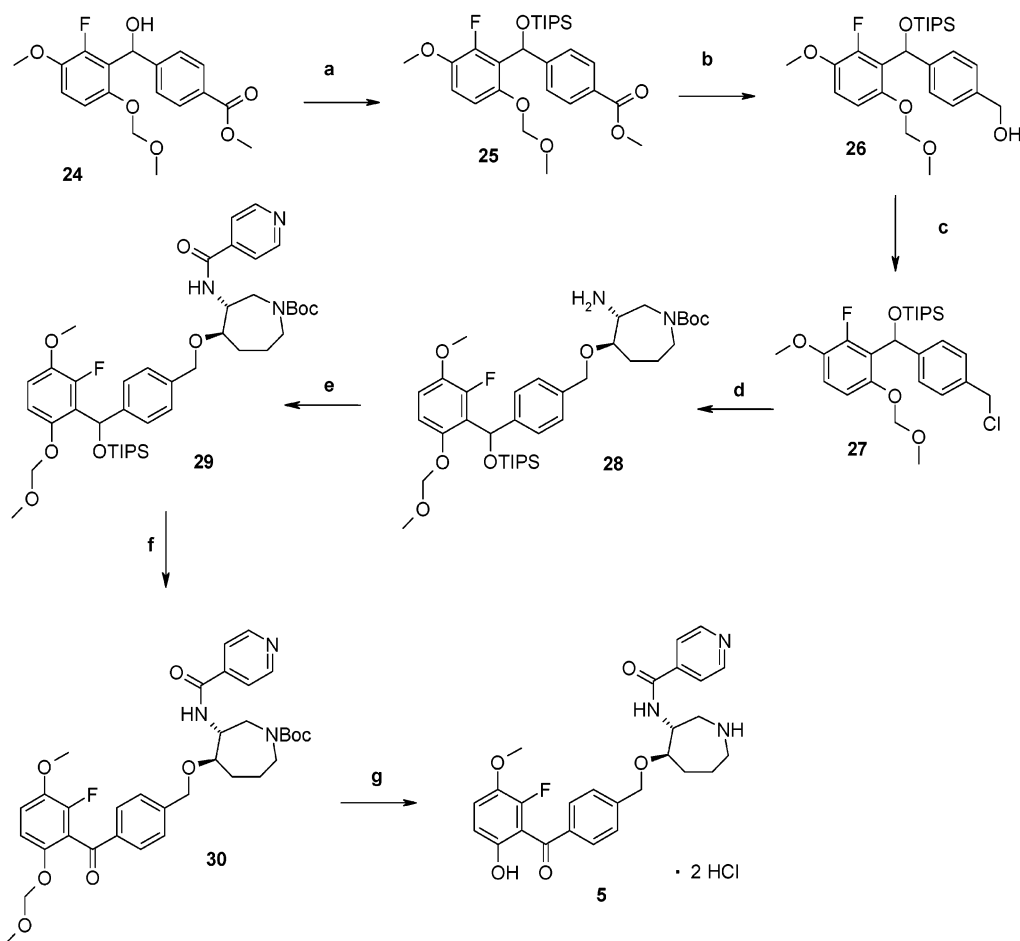
<sup>a</sup> Reagents and conditions: (a) NaCN, DMSO, 100 °C, 48 h, 57%; (b) Ra-Ni, 50 atm H<sub>2</sub>, CH<sub>3</sub>OH, 22%; (c) 4-iodobenzaldehyde **21**, n-BuLi, THF, -78 °C, 14 h, 50%; (d) MnO<sub>2</sub>, CH<sub>2</sub>Cl<sub>2</sub>, rt, 24 h, 95%; (e) **19**, 18-crown-6, t-BuOK, Pd<sub>2</sub>(dba)<sub>3</sub>, BINAP, THF, 15 h, reflux, 10%; (f) 4 M HCl in dioxane, rt, 15 h, 70%.

ably because the ether bond has to rearrange in order to adopt the trans binding conformation. A NOESY spectrum of **5** in D<sub>2</sub>O was obtained to analyze its conformation in water (Figure 3). The NOE between the pyridine protons H-C(3,5) and the benzoyl protons H-C(3',5') as well as the NOE between the pyridine protons H-C(2,6) and the benzoyl protons H-C(2',6') indicate that the unbound state of the molecule is stabilized by hydrophobic collapse. Hydrophobic collapse could stabilize the ligand in two ways. On one hand, it is favorable enthalpically, because the two terminal chromophores, pyridine and benzophenone, are brought into proximity for attractive  $\pi$ - $\pi$  interactions. On the other hand, this phenomenon is accompanied by desolvation of the molecule resulting in an entropy gain. In the collapsed conformation that molecule **5** adopts in solution, the pyridine is not in the right conformation to bind to the active site of PKB- $\alpha$  and, therefore, upon binding, significant reorganizational energy would be required, which is unfavorable for the binding free enthalpy of the ligand.

Molecule **7** (IC<sub>50</sub>(PKB- $\alpha$ ) = 2.8  $\mu$ M) is much less active than double amide **4** and ether **5**. A hypothetical interpretation of this result might be that the benzyl-amino linker in molecule **7** is more flexible and presumably not preorganized in the trans conformation in aqueous solution, and therefore a loss in entropy would occur upon binding. Furthermore, the amine is hydrophilic and basic and therefore protonated and hydrated in aqueous solution, and upon binding, dehydration (depends on protein) and deprotonation energy would

be required, which is unfavorable for the binding free enthalpy of the ligand as well. According to molecular modeling a protonated amine would result in steric hindrance between the ammonium protons and the ring protons of the azepane ring. Compound **6** is inactive (IC<sub>50</sub> = 25.8  $\mu$ M) which was predicted by modeling and is mainly due to steric hindrance between the methylene protons and the ring protons of the azepane ring which do not allow the linker to adopt the right conformation for binding of the different moieties of the molecule to their binding pockets.

**Crystallographic Results.** The inhibitors **4**, **5**, and **8** could be cocrystallized with PKA and were overlaid with the ester **1** as shown in Figure 4. The crystal structures reveal the conformations of the aforementioned inhibitors which differ only in the chemical entity of the linker between the azepane and benzophenone moieties in the bound state. It can be seen that inhibitors **4**, **5**, and **8** bind practically in the same conformation as the ester **1**. The conformation of the linker for which the torsional angle is *antiperiplanar* in all molecules is trans with respect to azepane and benzophenone. This confirms our modeling hypothesis that this is the favorable binding confirmation, because it orients the azepane and the benzophenone toward their binding pockets. Therefore, molecules which are preorganized in aqueous solution in the trans conformations have higher binding affinities which is in accordance with the biochemical data (see Table 2). In the complex between the double amide **4** and PKA (Figure 5a) there is a rearrangement of the side chains of Asp184, Thr183,

Scheme 3<sup>a</sup>

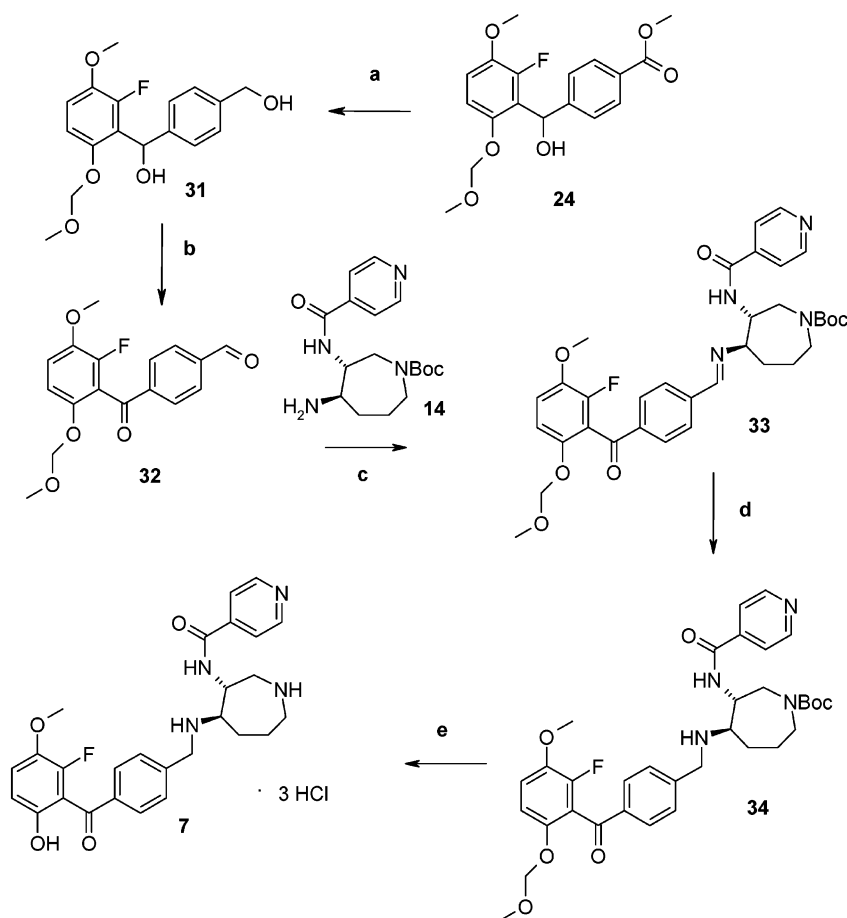
<sup>a</sup> Reagents and conditions: (a) imidazole, TIPS-Cl, DMF, rt, 15 h, then TIPSOSO<sub>2</sub>CF<sub>3</sub>, 100 °C, 36 h, 90%; (b) LiAlH<sub>4</sub>, THF, rt, 3.5 h, 70%; (c) PPh<sub>3</sub>, CCl<sub>4</sub>, rt, 3.5 h, 74%; (d) (3*R*, 4*S*)-3-amino-4-hydroxy-azepane-1-carboxylic acid *tert*-butyl ester 9, NaH, THF, reflux, 2 h, 43%; (e) isonicotinic acid 10, DCC, DMAP, CH<sub>2</sub>Cl<sub>2</sub>, rt, 15 h, 92%; (f) Bu<sub>4</sub>NF, THF, rt, 15 h, then MnO<sub>2</sub>, CH<sub>2</sub>Cl<sub>2</sub>, rt, 24 h, 72%; (g) 4 M HCl in dioxane, rt, 15 h, 91%.

and Lys72 compared to the complex of the ester with PKA as can be seen in Figure 4 and Figure 5a. In the complex of the double amide with PKA, the NH of the amide moiety (next to the benzophenone) of molecule 4 forms an OCNH...OOC hydrogen bond with the side chain of Asp184 (Table 3). Furthermore, Asp184 makes a COO...HN H-bond to the NH<sub>2</sub><sup>+</sup> of the azepane, and two more hydrogen bonds to the NH<sub>3</sub><sup>+</sup> of Lys72 and a water molecule. Thr183 makes an OH...OCNH H-bond with its side chain OH to the carbonyl oxygen of the amide next to pyridine in the inhibitor 4. Lys72 forms an additional NH...OH H-bond with its NH<sub>3</sub><sup>+</sup> to the inhibitor hydroxyl group of the benzophenone as compared to the complex of the ester 1 and PKA. These extra hydrogen bonding contacts between inhibitor and protein detected in the crystal structure of the complex of double amide 4 with PKA might contribute to its slightly higher binding affinity of IC<sub>50</sub> (PKA) = 2 nM compared to the ester (IC<sub>50</sub> (PKA) = 4 nM). In the cocrystal structure of the ether 5 with PKA (Figure 5b) Lys72 forms an additional NH...OH H-bond with its NH<sub>3</sub><sup>+</sup> to the inhibitor hydroxyl group of the benzophenone as compared to the complex of the ester 1 and PKA. Thr183 adopts two conformations in the same crystal: one as observed in the crystal structure of the complex of PKA with the ester 1, the other one as observed in the crystal structure of the complex with

the double amide 4. All other intermolecular bonding contacts are practically the same as described for the complex between PKA and the ester 1 (see Figure 2b).

Analysis of the crystal structure of the complex of the compound with the vinyl linker 8 with PKA (Figure 5c) reveals no significant changes in intermolecular binding contacts compared to the ester 1 except for an additional NH...OH H-bond between Lys72 with its NH<sub>3</sub><sup>+</sup> to the inhibitor hydroxyl group of the benzophenone. However, analysis of the crystal structure does not provide an explanation of its lower binding affinity of IC<sub>50</sub>(PKA) = 360 nM (Table 2).

**Conclusions.** Based upon molecular modeling studies on the X-ray crystal structure of the complex between the lead molecule 1 and PKA, new linkers isosteric to the plasma unstable ester were designed and introduced into 1 to give the compounds 4, 5, 6, 7, and 8. The *in vitro* PKA and PKB- $\alpha$  inhibitory activities of these molecules as inhibitors were measured and evaluated with respect to the modeling predictions. No significant differences in binding affinities for PKA and PKB- $\alpha$  could be observed. The binding affinities are in agreement with the modeling predictions for inhibitors 4, 5, 6, and 7. This confirms our hypothesis that PKA is a suitable surrogate kinase for PKB, and crystal structures of inhibitors cocrystallized with the kinase domain of PKA can be used for molecular modeling

Scheme 4<sup>a</sup>

<sup>a</sup> Reagents and conditions: (a)  $\text{LiAlH}_4$ , THF, rt, 3 h, 63%; (b)  $\text{MnO}_2$ ,  $\text{CH}_2\text{Cl}_2$ , rt, 22 h, 69%; (c) **14**,  $\text{C}_2\text{H}_5\text{OH}$ , reflux, 15 h, 95%; (d)  $\text{NaBH}_3\text{CN}$ ,  $\text{CH}_3\text{OH}$ , rt, 1 h, 57%; (e) 4 M HCl in dioxane, rt, 15 h, 57%.

studies for a design of active PKB- $\alpha$  inhibitors. This opens the possibility for further homology modeling studies with PKA as a model for PKB. It also allows the design of inhibitors which are selective for PKB- $\alpha$  against PKA, because there are different amino acids in PKB- $\alpha$  in a deeper pocket close to the benzophenone binding site in PKA which is not occupied by the aforementioned inhibitors. These studies also confirm the validity of selectivity predictions based on the X-ray structures of inhibitors cocrystallized with PKA/B mutant protein constructs and will be published separately.<sup>36,53a</sup> Based upon the available structures, it is also possible to design molecules that belong to completely different chemical classes as PKB- $\alpha$  inhibitors. Results of this approach will be published separately.<sup>53b</sup>

It was also shown that inhibitors **4**, **5**, and **7** are plasma stable analogues of the original lead **1**.<sup>1</sup> Inhibitor **4** had an inhibitory activity in the *in vitro* kinase assay on PKB- $\alpha$  of  $\text{IC}_{50} = 4$  nM and did not have the liability of plasma instability as the original lead. It was used as the new lead structure for further lead optimization of selectivity between PKB and PKA, bioavailability, and tolerability.

### Experimental Section

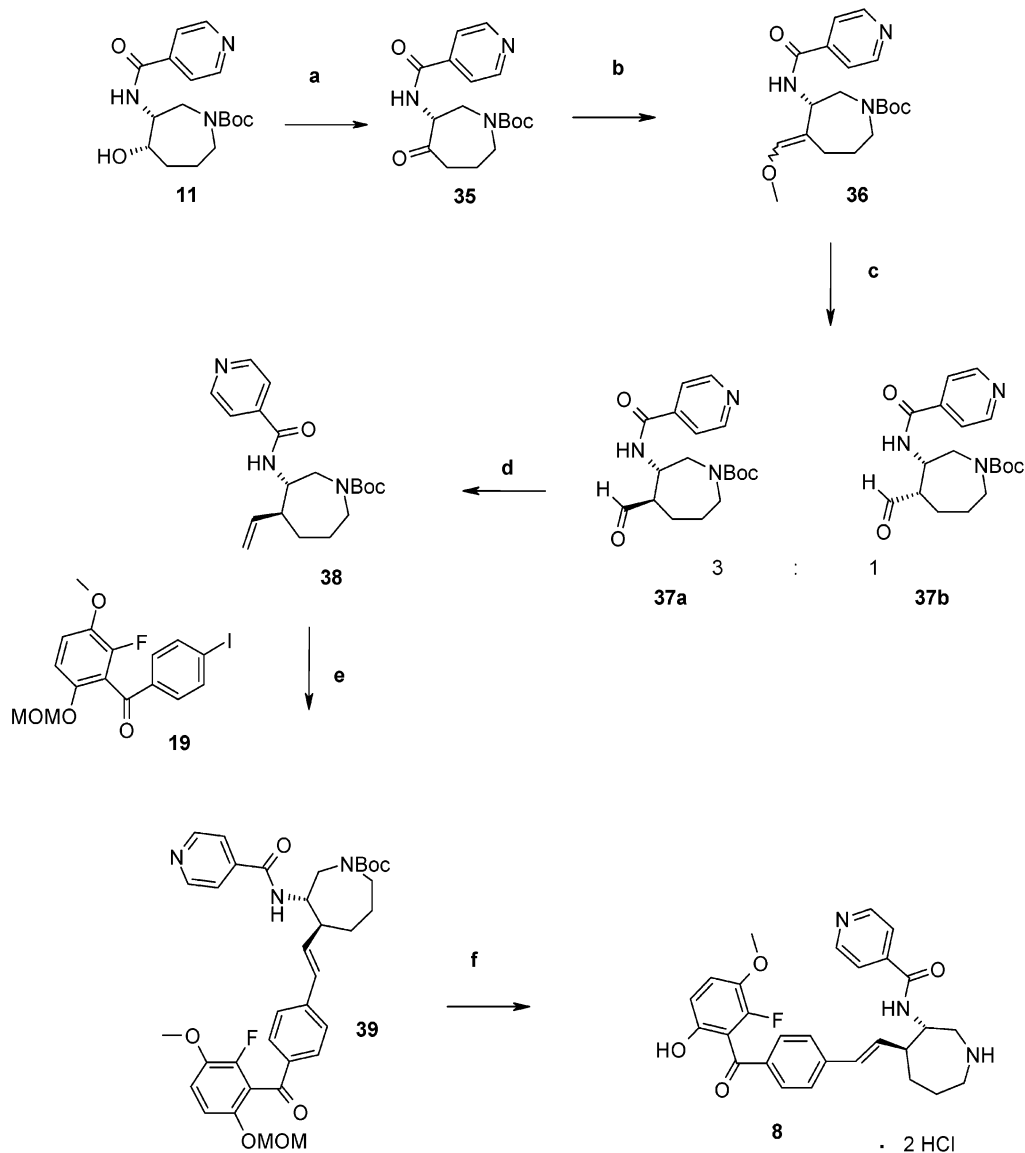
**Plasma Stability Assay.** To test the plasma stability of the inhibitors, mouse plasma tests have been used as follows:

Samples of mouse plasma containing each compound in a standard concentration (10  $\mu\text{mol/L}$ ) were prepared. After defined periods of time after the addition of said compounds

to the mouse plasma ( $t = 0, 0.5, 1, 2, 4$  h), equal portions were isolated from the plasma, separated with HPLC and analyzed by mass spectrometry. During all these steps, the temperature was kept constant at 37  $^\circ\text{C}$ .

**In Vitro Kinase Assays.** To study PKB- $\alpha$  inhibitory activity of the compounds, an ELISA-based assay has been developed for the serine/threonine kinase, PKB- $\alpha$ . The assay design utilizes an N-terminally biotinylated substrate peptide. When this substrate is phosphorylated by the PKB- $\alpha$  kinase, the product is recognized by a substrate/sequence-specific antibody known to bind to particular phosphorylated serine residues. For this assay a Biotin-SGRARTSSFAEPG peptide and anti-phospho-GSK-3 $\alpha$  Ser21 antibody (rabbit) from Cell Signaling Technology/New England Biolabs have been used.

The enzymatic reactions were carried out with PKB- $\alpha$  expressed in Sf9 cells (7.7 ng/reaction), substrate peptide (200 nM), and ATP (5  $\mu\text{M}$ ) in the absence or presence of different concentrations of compounds dissolved in DMSO. The final concentration of DMSO was 4%. The mixtures were reacted for 30 min at room temperature in assay buffer containing 50 mM Tris-HCl, 10 mM  $\text{MgCl}_2$ , 1.0 mM DTT, 0.2 mM  $\text{Na}_3\text{VO}_4$ , pH 7.5, in a final volume of 50  $\mu\text{L}$ . The reaction was stopped by addition of 10  $\mu\text{L}$  0.12 M EDTA/0.12 M EGTA. The reaction mixture was transferred to a SA-coated microtiter plate. After 1 h incubation, the plate was washed with PBS using a 384-well Embla plate washer. Anti-phospho-GSK-3 $\alpha$  Ser21 antibody was added. After 1 h incubation, the plate was washed with PBS and bound antibody was detected by addition of polyclonal <rabbit>S-IgG-POD conjugate from Roche Diagnostics GmbH. After 1 h incubation, the plate was washed with PBS. The amount of phosphorylated peptide was measured by the enzyme-catalyzed ABTS (ABTS is a trademark of a

Scheme 5<sup>a</sup>

<sup>a</sup> Reagents and conditions: (a) ClCOCOCl, DMSO, CH<sub>2</sub>Cl<sub>2</sub>, Et<sub>3</sub>N, -78 °C, 30 min, 85%; (b) Ph<sub>3</sub>P<sup>+</sup>CH<sub>2</sub>OCH<sub>3</sub>Cl<sup>-</sup>, KO<sup>t</sup>Bu, Et<sub>2</sub>O, -30 °C to 0 °C, 59%; (c) Cl<sub>3</sub>CCOOH, CHCl<sub>3</sub>, reflux, 1 h, 68%; (d) n-BuLi, Ph<sub>3</sub>P<sup>+</sup>CH<sub>3</sub>I<sup>-</sup>, THF, -78 °C to rt, 14 h, 50%; (e) **19**, Pd(OAc)<sub>2</sub>, (o-Tol)<sub>3</sub>P, *N,N*-diisopropylamine, DMF, 105 °C, 14 h, 20%; (f) 2 M HCl in diethyl ether, rt, 15 h, 97%.

member of the Roche group) conversion and photometrical measurement at 405 nm.

To determine IC<sub>50</sub> values, the compounds were tested in the concentration range from 100 μM to 20 pM. Calculation of IC<sub>50</sub> values were performed with ActivityBase.

To study PKA inhibitory activity of the compounds, a fluorescence polarization-based assay (Protein Kinase C Assay Kit, Green, PanVera), which is also suitable for the serine/threonine kinase PKA, was used. In this assay, a fluorescent phosphopeptide tracer and the nonfluorescent phosphopeptides generated during a PKA reaction compete for binding to an antiphosphoserine antibody. In a reaction mixture containing no phosphopeptide product, the fluorescent tracer is bound by the antibody, and the emission signal is polarized. However, in a reaction mixture containing phosphopeptide product, the fluorescent tracer is displaced from the antibody and the emission signal becomes depolarized. Different concentrations of compounds dissolved in DMSO (max. final DMSO concentration 2.5%) were incubated with PKA- $\alpha$  enzyme (recombinant from *E. coli*, 10 ng/reaction) together with PKC buffer, PKC peptide substrate (2 μM), and PKC tracer (all from PanVera) as well as 9 mM Hepes-buffer pH 7.2, 0.05% Nonidet-P40, and 50 μM Na<sub>3</sub>VO<sub>4</sub> for 30 min at room temper-

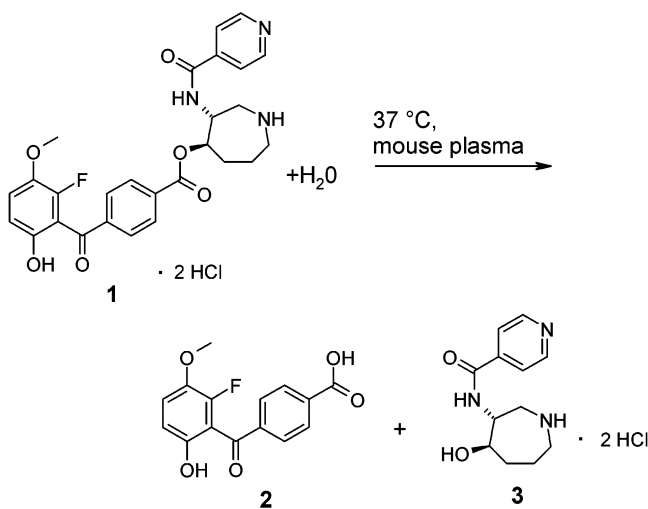
ature. The kinase reaction was started subsequently by adding ATP (5.76 μM final concentration) and incubated for 90 min at room temperature. Finally, the reaction was stopped by adding the same volume of a 1:1 mixture of quenching buffer and phosphoserine antibody (both from PanVera). After another 30 min of incubation, enzymatic activity was measured by detection of fluorescence polarity in a Victor 2 reader (Wallac, Finland).

To determine IC<sub>50</sub> values, the compounds were tested in the concentration range from 100 μM to 20 pM. Calculation of IC<sub>50</sub> values were performed with ActivityBase.

**Protein Expression and Purification.** Recombinant bovine  $\alpha$  catalytic subunit of cAMP dependent protein kinase (PKA) (which differs from the human protein at two positions: N32S and M63K) was solubly expressed in *E. coli* BL21-(DE3) cells and then purified via affinity chromatography and ion exchange chromatography as previously described.<sup>42,43</sup> Heterogeneously phosphorylated PKA was used for the kinase assay. Three fold phosphorylated protein was used for crystallization of all inhibitors.

**Crystallization.** The inhibitors **1**, **4**, **5**, and **8** were cocrystallized with PKA and PKI(5–24) at 75 mM LiCl, 25 mM MesBisTris, pH 6.4. Hanging drop vapor diffusion method



**Table 1.** Half-Lives of Inhibitors in Mouse Plasma at 37 °C


inhibitor	$T_{1/2}$
<b>1</b>	< 1 min
<b>4</b>	69 h
<b>5</b>	29 h
<b>7</b>	161 h

**Table 2.** IC<sub>50</sub> Values Measured for Binding of Inhibitors to PKB- $\alpha$  and PKA

inhibitor	IC <sub>50</sub> (PKB- $\alpha$ )	IC <sub>50</sub> (PKA)
<b>1</b>	5 nM	5 nM
<b>4</b>	4 nM	2 nM
<b>5</b>	355 nM	39 nM
<b>6</b>	25 $\mu$ M	45 $\mu$ M
<b>7</b>	3 $\mu$ M	800 nM
<b>8</b>	160 nM	360 nM

against 15% methanol as precipitant was used to obtain ca. 100  $\times$  100  $\times$  500  $\mu$ m crystals.

**Data Collection and Structure Determination.** Diffraction data were measured at 4 °C in a sealed capillary on an image plate detector (Mar research) or Bruker  $\times$ 1000 area detector using a copper target Rigaku Rotaflex X-ray generator and graphite crystal monochromator. In each case one crystal was sufficient to obtain a complete data set. In case of compound **8**, the crystals were flash frozen in liquid nitrogen and measured at the synchrotron beamline BW-6 at the DESY (Hamburg, Germany). The data were processed with the program MOSFLM and SCALA or ASTRO and SAINT. All crystals have orthorhombic symmetry ( $P2_12_12_1$ ) with nearly the same cell constants.

The structures were determined by molecular replacement using the CCP4 program package ([www.ccp4.ac.uk/main/html](http://www.ccp4.ac.uk/main/html)). As a starting model, we chose a PKA structure in a closed conformation (to be published). Refmac 5.1.24 was used for refinement, while MOLOC<sup>46</sup> ([www.moloc.ch](http://www.moloc.ch)) was used for graphical evaluation and model building. The structures are depicted in the Figures 1, 2a,b, 4, and 5a–c with graphics from programs MOLSCRIPT,<sup>54</sup> BOBSCRIPT,<sup>54–56</sup> and Raster3d.<sup>57,58</sup>

**Data Deposition.** Atomic coordinates have been deposited in the Protein Data Bank.

**Molecular Modeling.** The design of target molecules with different linkers between the azepane and benzophenone part of lead molecule **1** was carried out on a Silicon Graphics Octane workstation. The starting geometries for the molecular mechanics studies were constructed with the program MOLOC, from crystallographic data and standard molecular fragments. The proposed inhibitor was minimized separately and docked manually into its expected binding site. The coordinates of PKA were constrained. The inhibitors were minimized inside the enzyme. Energy minimizations were performed in vacuo by MOLOC with the MAB force field. The energy was

minimized by conjugate gradients to a final value of the sum of the squares of the components of the gradient of less than the accuracy (0.1 or relative value of 1).

**(3R,4S)-4-Hydroxy-3-[(pyridine-4-carbonyl)-amino]-azepane-1-carboxylic Acid *tert*-Butyl Ester (**11**).** A solution of compound **9**<sup>48</sup> (4.60 g, 20.0 mmol), isonicotinic acid (2.46 g, 20.0 mmol) and DMAP (1.22 g, 10.0 mmol) in anhydrous CH<sub>2</sub>Cl<sub>2</sub> (100 mL) was cooled to 0 °C. A solution of DCC (4.13 g, 20.0 mmol) in anhydrous CH<sub>2</sub>Cl<sub>2</sub> (50 mL) was added dropwise. The resulting mixture was stirred for 24 h at room temperature. Water (30 mL) was added, and stirring was continued for 30 min. After filtration and separation, the organic layer was washed with water (2  $\times$  20 mL), and the aqueous layers were re-extracted with CH<sub>2</sub>Cl<sub>2</sub> (2  $\times$  20 mL). The combined organic layers were washed with brine and dried over Na<sub>2</sub>SO<sub>4</sub>. After filtration and evaporation, the residue was purified by column chromatography on silica gel (column, 3 cm  $\times$  25 cm; eluent, ethyl acetate:CH<sub>3</sub>OH = 97:3). A yellow oil was obtained (6.6 g, 98%).  $[\alpha]_D^{20}$  14.2° (*c* 0.6, CHCl<sub>3</sub>). IR:  $\nu$  (cm<sup>-1</sup>) = 1666, 1415, 1165. <sup>1</sup>H NMR (250 MHz, CDCl<sub>3</sub>):  $\delta$  1.44 (s, 9H), 1.50–1.95 (m, 4H), 2.83–3.12 (m, 2H), 3.67–3.87 (m, 1H), 3.89–4.15 (m, 2H), 4.37 (br s, 1H), 4.65 (br s, 1H), 7.51–7.72 (m, 2H), 8.40 (br s, 1H), 8.62–8.73 (m, 2H). <sup>13</sup>C NMR (62.5 MHz, CDCl<sub>3</sub>):  $\delta$  20.79, 27.36, 46.63, 47.29, 56.20, 59.40, 72.98, 80.01, 120.09, 139.50, 149.52, 157.20, 166.54. MS (70 eV), *m/z* (%): 336 (30, M<sup>+</sup> + 1), 123 (100); HR-MS (ESI): calcd for C<sub>17</sub>H<sub>26</sub>N<sub>3</sub>O<sub>4</sub> [M + H]: 336.1923; found: 336.1968.

**(3R,4S)-4-Methanesulfonyloxy-3-[(pyridine-4-carbonyl)-amino]-azepane-1-carboxylic Acid *tert*-Butyl Ester (**12**).** A solution of **11** (6.60 g, 19.7 mmol) in anhydrous pyridine (100 mL) was cooled to 0 °C. Methanesulfonic acid chloride (6.76 g, 59.0 mmol) was added during 1 h. The mixture was stirred for 24 h at room temperature, and the volatile components were removed in vacuo. The residue was dissolved in ethyl acetate/water (200 mL, 1:1), and the aqueous layer was extracted with ethyl acetate (3  $\times$  30 mL). The combined organic layers were washed with brine and dried over Na<sub>2</sub>SO<sub>4</sub>. After filtration and evaporation, the residue was purified by column chromatography on silica gel (column, 5 cm  $\times$  35 cm; eluent, (1) ethyl acetate, (2) ethyl acetate/CH<sub>3</sub>OH = 99:1, (3) ethyl acetate/CH<sub>3</sub>OH = 97:3). A yellow oil was obtained (6.4 g, 79%). <sup>1</sup>H NMR (250 MHz, CDCl<sub>3</sub>):  $\delta$  1.39 (s, 9H), 1.55–2.35 (m, 4H), 2.78–2.95 (br s, 3H), 2.90–3.82 (m, 4H), 4.35–4.55 (m, 1H), 5.12–5.19 (m, 1H), 6.82 (br d, 0.3H), 7.58–7.65 (m, 2H), 7.90–8.05 (br d, 0.7H), 8.62–8.76 (m, 2H). <sup>13</sup>C NMR (62.5 MHz, CDCl<sub>3</sub>):  $\delta$  21.09, 27.36, 28.11, 36.99, 47.12, 51.30, 52.06, 59.39, 79.40, 119.93, 139.83, 149.65, 156.20, 163.56. MS (70 eV), *m/z* (%): 414 (100, M<sup>+</sup> + 1); HR-MS (ESI): calcd for C<sub>18</sub>H<sub>28</sub>N<sub>3</sub>O<sub>6</sub>S [M + H]: 414.1699; found: 414.1726.

**(3R,4R)-4-Azido-3-[(pyridine-4-carbonyl)-amino]-azepane-1-carboxylic Acid *tert*-Butyl Ester (**13**).** Compound **12** (21.5 g, 52.0 mmol) was dissolved in DMF (500 mL), and sodium azide (16.9 g, 26.0 mmol) was added. The mixture was stirred for 3 h at 90 °C. Another portion of sodium azide (16.9 g, 26.0 mmol) was added, the mixture was stirred for 3 h at 90 °C and for 24 h at room temperature, and the solvent was evaporated. The residue was dissolved in ethyl acetate/water (200 mL, 1:1), and the aqueous layer was extracted with ethyl acetate (3  $\times$  30 mL). The combined organic layers were washed with brine and dried over Na<sub>2</sub>SO<sub>4</sub>. After filtration and evaporation, the residue was purified by column chromatography on silica gel (column, 5 cm  $\times$  35 cm; eluent, ethyl acetate/heptane = 9:1). A yellow oil was obtained (17.0 g, 91%). <sup>1</sup>H NMR (250 MHz, CDCl<sub>3</sub>):  $\delta$  1.39 (s, 9H), 1.55–2.01 (m, 4H), 2.82–2.93 (m, 1H), 3.12–3.24 (m, 1H), 3.72–3.85 (m, 1H), 3.94–4.24 (m, 3H), 7.63 (d, <sup>3</sup>*J* = 5.2 Hz, 2H), 8.41 (br s, 1H), 8.62 (d, <sup>3</sup>*J* = 5.2 Hz, 2H). <sup>13</sup>C NMR (62.5 MHz, CDCl<sub>3</sub>):  $\delta$  26.17, 28.76, 30.01, 36.87, 48.19, 55.59, 62.56, 81.48, 121.32, 141.35, 150.94, 158.65, 162.91. MS (70 eV), *m/z* (%): 359 (22, M<sup>+</sup> - 1), 259 (100).

**(3R,4R)-4-Amino-3-[(pyridine-4-carbonyl)-amino]-azepane-1-carboxylic Acid *tert*-Butyl Ester (**14**).** Compound **13** (17.0 g, 47.2 mmol) dissolved in CH<sub>3</sub>OH (850 mL) was hydrogenated (anhydrous Ra–Ni (7 g), 1 bar). The mixture

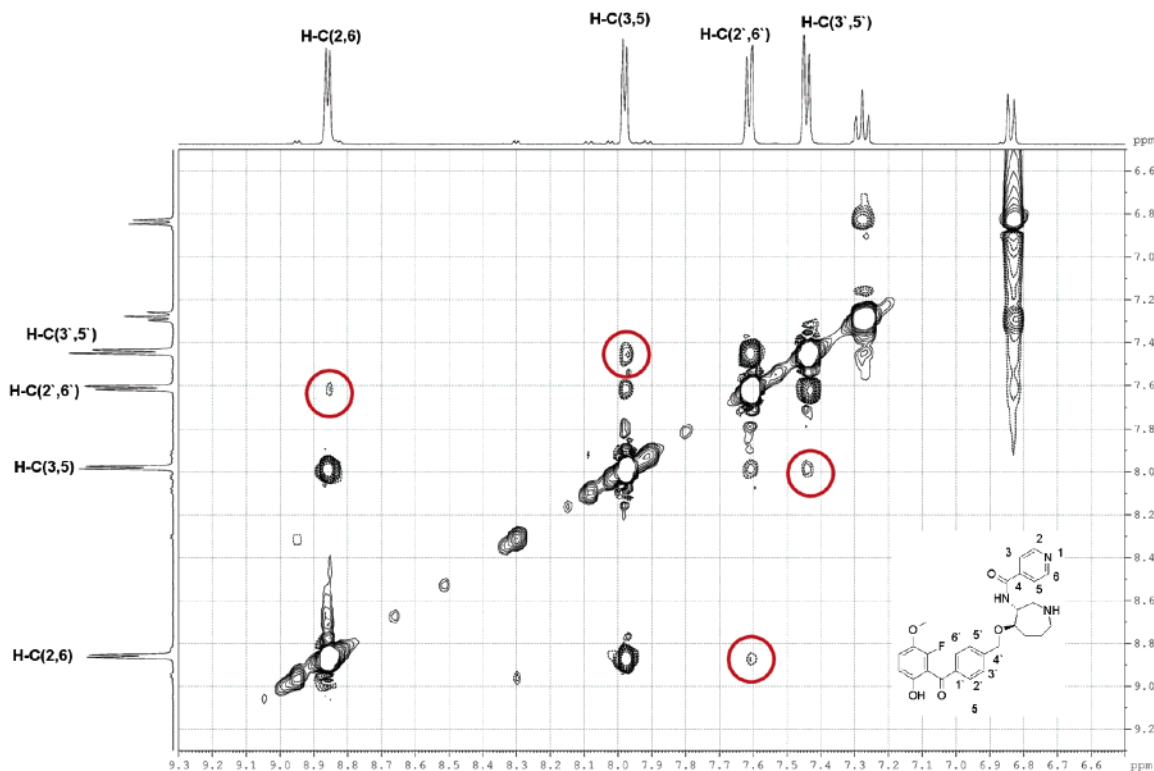


**Figure 3.**  $^1\text{H}$  NMR ( $\text{D}_2\text{O}$ , 500 MHz) NOESY spectrum of **5**. The NOE between the pyridine protons H-C(3,5) and the benzoyl protons H-C(3',5') as well as the NOE between the pyridine protons H-C(2,6) and the benzoyl protons H-C(2',6') indicate that the unbound state of the molecule is stabilized by hydrophobic collapse.

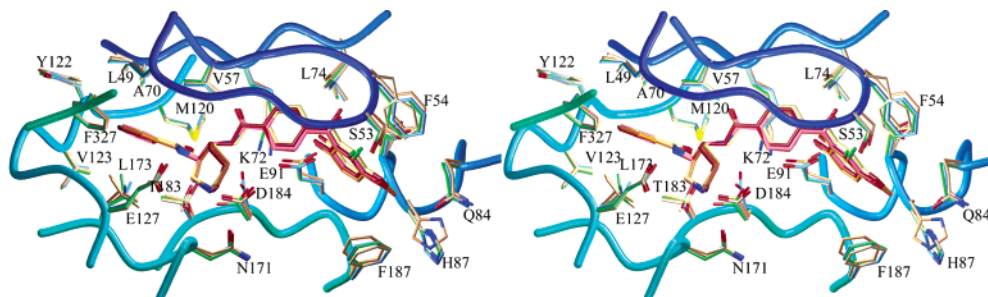


**Figure 4.** Overlay of X-ray crystal structures of inhibitors **1**, **4**, **5**, and **8** situated in the active site of PKA. The protein backbone ribbon with conformation of side chains relevant for binding interactions with the inhibitors is shown.

was filtered carefully, and the volatile components were removed in vacuo. The residue was solvated in ethyl acetate (200 mL), dried over  $\text{Na}_2\text{SO}_4$ , filtered, and evaporated to yield a light brown amorphous compound (16.5 g, 95%).  $[\alpha]_{\text{D}}^{20} -27.1^\circ$  ( $c$  0.6,  $\text{CHCl}_3$ ). IR:  $\nu$  ( $\text{cm}^{-1}$ ) = 1665, 1417, 1163.  $^1\text{H}$  NMR (400 MHz, DMSO):  $\delta$  1.37 (s, 6H), 1.42 (s, 3H), 1.45–1.74 (m, 2H), 1.71–1.92 (m, 2H), 2.72–2.88 (m, 1H), 3.05–3.30 (m, 2H), 3.28–3.44 (br s, 2H), 3.45–3.65 (m, 2H), 3.73 (br s, 1H), 7.74 (d,  $^3J = 5.0$  Hz, 0.6H), 7.78 (d,  $^3J = 5.8$  Hz, 1.4H), 8.29–8.38 (br s, 1H), 8.70–8.76 (m, 2H).  $^{13}\text{C}$  NMR (62.5 MHz,  $\text{CDCl}_3$ ):  $\delta$  25.44, 27.40, 31.67, 45.00, 49.01, 56.25, 57.89, 79.71, 119.99, 140.36, 149.53, 156.71, 164.16. MS (70 eV),  $m/z$  (%): 334 (100, M).

**(3R,4R)-4-[4-(2-Fluoro-3-methoxy-6-methoxymethoxy-benzoyl)-benzoylamino]-3-[(pyridine-4-carbonyl)-amino]-azepane-1-carboxylic Acid *tert*-Butyl Ester (**16**).** 4-(2-Fluoro-3-methoxy-6-methoxymethoxy-benzoyl)-benzoic acid (**15**)<sup>35</sup> (176 mg, 0.50 mmol), DMAP (31 mg, 0.30 mmol), and DCC (113 mg, 0.55 mmol) were added to a solution of **14** (167 mg, 0.50 mmol) in  $\text{CH}_2\text{Cl}_2$  (5 mL). The mixture was stirred for 6 h at room temperature and filtered. The filter cake was washed with  $\text{CH}_2\text{Cl}_2$  ( $3 \times 4$  mL), and the combined organic layers were washed with water ( $2 \times 3$  mL). After drying over  $\text{Na}_2\text{SO}_4$ , filtration, and concentration in vacuo, the residue was

purified by column chromatography on silica gel (column, 2 cm  $\times$  20 cm; eluent, ethyl acetate). An amorphous colorless compound was obtained (240 mg, 76%, mp: 105–107  $^\circ\text{C}$ ).  $^1\text{H}$  NMR (400 MHz, DMSO):  $\delta$  1.41 (s, 6H), 1.45 (s, 3H), 1.55–2.05 (m, 4H), 3.05 (s, 3H), 3.05–3.26 (m, 2H), 3.45–3.70 (m, 2H), 3.84 (s, 3H), 4.09–4.23 (m, 2H), 5.02 (s, 2H), 7.03 (d,  $^3J = 7.8$  Hz, 1H), 7.28 (t,  $^3J = 8.0$  Hz, 1H), 7.55 (d,  $^3J = 5.4$  Hz, 1H), 7.59 (d,  $^3J = 5.5$  Hz, 1H), 7.74–7.83 (m, 4H), 8.53–8.71 (m, 4H). MS (70 eV),  $m/z$  (%): 650 (80, M+), 649 (100); HR-MS (ESI): calcd for  $\text{C}_{34}\text{H}_{40}\text{N}_4\text{O}_8\text{F}$  [M + H]: 651.2830; found: 651.2841.

**(3R,4R)-N-{4-[4-(2-Fluoro-6-hydroxy-3-methoxy-benzoyl)-benzoylamino]-azepan-3-yl}-isonicotinamide Hydrochloride (**4**).** HCl in dioxane (4 M, 2 mL, 8.0 mmol) was added to a solution of **16** (260 mg, 0.42 mmol) in anhydrous dioxane (2 mL). The mixture was stirred for 15 h at room temperature, and the resulting light yellow crystals were separated (185 mg, 78%, mp: 200  $^\circ\text{C}$  dec). The purity of the compound was determined as 99.3% by analytical HPLC.  $^1\text{H}$  NMR (500 MHz, DMSO):  $\delta$  1.85–2.10 (m, 4H), 3.07 (br s, 1H), 3.24 (br s, 1H), 3.32–3.45 (m, 2H), 3.80 (s, 3H), 4.32–4.40 (m, 1H), 4.47–5.56 (m, 1H), 6.74 (d,  $^3J = 7.8$  Hz, 1H), 7.18 (t,  $^3J = 7.9$  Hz, 1H), 7.76 (d,  $^3J = 8.3$  Hz, 2H), 7.84 (d,  $^3J = 5.3$  Hz, 2H), 8.05 (d,  $^3J = 8.3$  Hz, 2H), 8.85–8.92 (m, 3H), 9.31 (m,

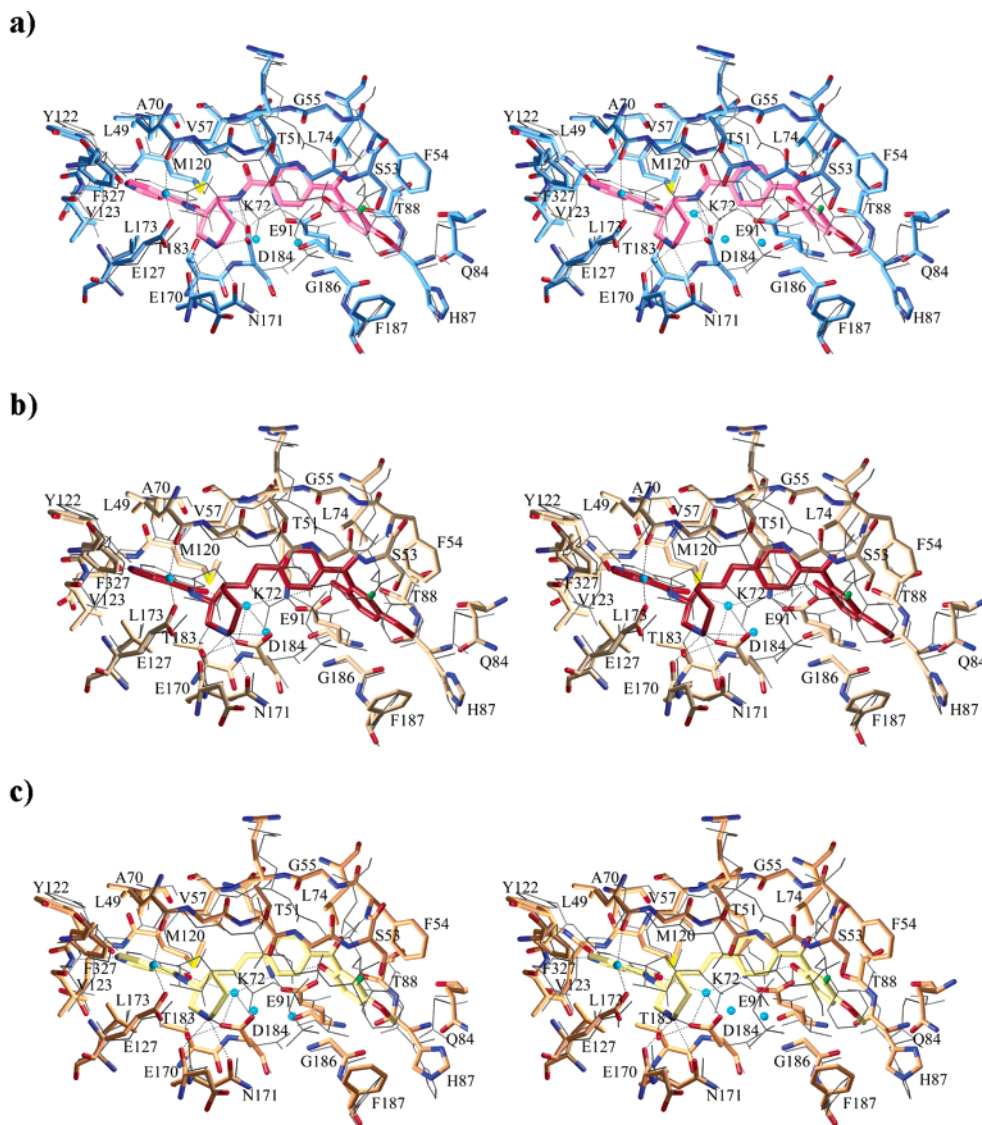


**Figure 5.** X-ray crystal structures of PKA with inhibitor **4** (a), **5** (b), and **8** (c), respectively, were superimposed with the AMP-PNP complex (1CDK). The figures show the binding mode in the active site of PKA. The hydrogen bonds between the inhibitors and the amino acids of PKA and water molecules are indicated.

1H), 9.40 (br s, 1H), 9.68 (br s, 1H).  $^{13}\text{C}$  NMR (125 MHz, DMSO):  $\delta$  22.52, 30.09, 46.60, 47.31, 52.20, 54.13, 95.88, 111.56, 116.78, 123.93, 128.39, 129.36, 138.82, 139.73, 140.19, 140.28, 146.35, 148.06, 149.24, 150.01, 163.57, 165.98, 191.68. MS (70 eV),  $m/z$  (%): 507 (100,  $\text{M}^+ + 1$ ). HR-MS (ESI): calcd for  $\text{C}_{27}\text{H}_{28}\text{N}_4\text{O}_5\text{F}$  [M + H]: 507.2044; found: 507.2067.

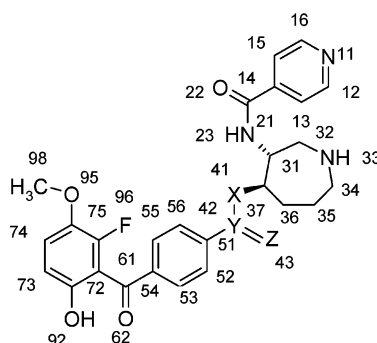
**(3R,4R)-4-Cyano-3-[(pyridine-4-carbonyl)-amino]-azepane-1-carboxylic Acid *tert*-Butyl Ester (17).** (3R,4S)-4-Methanesulfonyloxy-3-[(pyridine-4-carbonyl)-amino]-azepane-1-carboxylic acid *tert*-butyl ester (**12**) (103 mg, 0.25 mmol) and NaCN (122.5 mg, 2.50 mmol) in anhydrous DMSO (2 mL) were stirred for 48 h at 100 °C under argon. Water (20 mL) was added, and the suspension was extracted with ethyl acetate (3  $\times$  20 mL). The combined organic layers were washed with brine and dried over  $\text{Na}_2\text{SO}_4$ . After filtration and evaporation, the residue was purified by flash chromatography on silica gel (column, 2 cm  $\times$  15 cm; eluent, (1) ethyl acetate/heptane, (2) ethyl acetate to (3) ethyl acetate/ $\text{CH}_3\text{OH}$  = 95:5). A yellow gum was obtained (102 mg, 57%).  $^1\text{H}$  NMR (250 MHz,  $\text{CDCl}_3$ ):  $\delta$  1.35 (s, 3H), 1.42 (s, 6H), 1.55–2.00 (m, 4H), 2.95–3.07 (m, 1H), 3.15–3.25 (m, 1H), 3.55–4.35 (m, 4H), 7.55–7.68 (m, 2H), 8.60–8.72 (m, 3H).  $^{13}\text{C}$  NMR (62.5 MHz,  $\text{CDCl}_3$ ):  $\delta$  22.86, 27.33, 29.83, 30.98, 45.90, 48.59, 52.50, 80.54, 119.84, 139.32, 149.62, 164.18. MS (70 eV),  $m/z$  (%): 345 (100,  $\text{M}^+ + 1$ ).

**(3R,4S)-4-Aminomethyl-3-[(pyridine-4-carbonyl)-amino]-azepane-1-carboxylic Acid *tert*-Butyl Ester (18).**

Cyanide **17** (445 mg, 1.29 mmol) in  $\text{CH}_3\text{OH}$  (25 mL) and liquid ammonia (25 mL) was hydrogenated (anhydrous Ra-Ni (100 mg), 50 bar). The mixture was filtered carefully, and the volatile components were removed in vacuo. The residue was purified by flash chromatography on silica gel (column, 2 cm  $\times$  15 cm; eluent, (1)  $\text{CH}_2\text{Cl}_2/2\text{N NH}_3$  in  $\text{CH}_3\text{OH}$  = 99:1 to  $\text{CH}_2\text{Cl}_2/2\text{N NH}_3$  in  $\text{CH}_3\text{OH}$  = 90:10) to yield a light brown oil (100 mg, 22%).  $^1\text{H}$  NMR (250 MHz,  $\text{CDCl}_3$ ):  $\delta$  1.40 (s, 9H), 1.45–1.95 (m, 5H), 2.65–2.83 (m, 1H), 3.02–3.63 (m, 5H), 3.73–3.85 (m, 1H), 7.59 (d,  $^3J = 5.3$  Hz, 2H), 8.67 (d,  $^3J = 5.3$  Hz, 2H).  $^{13}\text{C}$  NMR (62.5 MHz,  $\text{CDCl}_3$ ):  $\delta$  22.98, 26.40, 29.57, 30.88, 43.44, 45.63, 46.62, 47.26, 78.95, 119.99, 140.85, 149.39, 155.38, 163.74. MS (70 eV),  $m/z$  (%): 349 (100,  $\text{M}^+ + 1$ ).

**(2-Fluoro-3-methoxy-6-methoxymethoxy-phenyl)-(4-iodo-phenyl)-methanol (22).** BuLi solution (1.6 M in hexane, 12.1 mL, 19.3 mmol) was added to a solution of 2-fluoro-1-methoxy-4-methoxymethoxybenzene **20** (2.4 g, 12.9 mmol) in anhydrous THF (30 mL) at  $-78$  °C. The solution was stirred for 40 min at  $-70$  °C and then added dropwise in a period of 20 min to a solution of 4-iodo-benzaldehyde **21** (4.49 g, 19.3 mmol) in anhydrous THF (25 mL) at  $-78$  °C. The mixture was warmed to room temperature in a period of 14 h. Water (20 mL) and ethyl acetate (20 mL) were added, and the separated aqueous layer was re-extracted with ethyl acetate (2  $\times$  40 mL). The combined organic layers were washed with brine and dried over  $\text{Na}_2\text{SO}_4$ . After filtration and evaporation, the residue was

Table 3. H-Bonds



H-bonds between		PKA Ester <b>1</b>	PKA amide <b>4</b>	PKA ether <b>5</b>	PKA vinyl <b>8</b>
inhibitor atom	protein atom	distance (Å)	distance (Å)	distance (Å)	distance (Å)
N11	Val123 (N)	3.3	3.2	3.1	3.1
O22	Thr183 (OG1)	—	2.8	[O]	—
N33	Asp184 (OD1)	2.9	2.7	2.5	2.9
N33	Asp184 (OD2)	3.4	3.4	3.3	—
N33	Glu170 (O)	2.9	2.9	3.1	2.9
N33	Asn171 (OD1)	3.1	2.9	3.2	3.1
X41	Asp184 (OD2)	—	3.0	—	—
X41	Asp184 (OD1)	—	3.4	—	—
O62	Phe54 (N)	3.1	3.0	3.3	2.0
O92	Glu91 (OE1)	2.5	2.6	2.7	2.7
O92	Lys72 (NZ)	—	3.1	3.1	3.2
inhibitor atom	water atom (connects to protein)	distance (Å)	distance (Å)	distance (Å)	distance (Å)
O22	X54–Lys72 (NZ)	2.9–2.6	2.9–3.4	2.8–2.8	3.1–2.9
	–Asp184 (OD1)	–2.5	–2.7	–3.2	–2.9
	–Asp184 (OD1)	–3.1	–	–2.9	–2.9
N23	X22–Glu127 (OE2)	2.9–2.6	2.9–2.7	3.1–2.7	3.1–2.6
	–Leu49 (O)	–3.0	–2.9	–3.0	–2.9

purified by flash chromatography on silica gel (column, 4 cm × 25 cm; eluent, ethyl acetate/heptane = 1:1) to yield a light-yellow oil (4.2 g, 50%). <sup>1</sup>H NMR (500 MHz, CDCl<sub>3</sub>): δ 3.27 (s, 3H), 3.80 (d, 1H), 3.87 (s, 3H), 4.98 (d, 1H), 5.07 (d, 1H), 6.18 (d, 1H), 6.85 (m, 2H), 7.12 (d, 2H), 7.64 (d, 2H). <sup>13</sup>C NMR (100 MHz, CDCl<sub>3</sub>): δ 56.25, 56.80, 67.79, 92.38, 95.04, 109.95, 112.85, 120.86, 127.54, 137.15, 143.07, 143.29, 148.77, 151.30. HR-MS (EI): calcd for C<sub>16</sub>H<sub>16</sub>FIO<sub>4</sub><sup>+</sup> [M]<sup>+</sup>: 418.0072; found: 418.0073.

**(2-Fluoro-3-methoxy-6-methoxymethoxy-phenyl)-(4-iodo-phenyl)-methanone (19)**. Carbinol **22** (300 mg, 0.72 mmol) was dissolved in anhydrous CH<sub>2</sub>Cl<sub>2</sub> (2 mL). Activated MnO<sub>2</sub> (350 mg) was added, and the mixture was stirred for 24 h. After filtration through a plug of Celite and evaporation, the residue was purified by flash chromatography on silica gel (column, 2 cm × 10 cm; eluent, ethyl acetate/heptane = 4:1) to yield a colorless oil (290 mg, 95%). <sup>1</sup>H NMR (500 MHz, CDCl<sub>3</sub>): δ 3.32 (s, 3H), 3.90 (s, 3H), 5.03 (s, 2H), 6.95 (d, 1H), 7.02 (t, 1H), 7.59 (d, 2H), 7.84 (d, 2H). <sup>13</sup>C NMR (100 MHz, CDCl<sub>3</sub>): δ 56.22, 57.09, 95.32, 102.19, 110.67, 115.29, 119.42, 130.88, 136.40, 137.98, 142.98, 148.22, 150.49, 190.70. HR-MS (EI): calcd for C<sub>16</sub>H<sub>14</sub>FIO<sub>4</sub><sup>+</sup> [M]<sup>+</sup>: 415.9915; found: 415.9926.

**(3R,4S)-N-(4-{[4-(2-Fluoro-3-methoxy-6-methoxymethoxy-benzoyl)-phenylamino]-methyl}-3-{(pyridine-4-carbonyl)-amino]-azepan-1-carboxylic Acid *tert*-Butyl Ester (23)**. 18-crown-6 (84.0 mg, 0.32 mmol), aryl iodide **19** (60.0 mg, 0.15 mmol), amine **18** (45.0 mg, 0.15 mmol), <sup>t</sup>BuOK (31.0 mg, 0.32 mmol), Pd<sub>2</sub>(dba)<sub>3</sub> (5.2 mg), and BINAP (10.8 mg) were added to anhydrous THF (0.5 mL), and the mixture was stirred for 15 h at reflux. The volatile components were evaporated in vacuo, and the residue was purified by flash chromatography on silica gel (column, 1.5 cm × 15 cm; eluent, ethyl acetate/MeOH = 19:1) to yield a dense colorless oil (12 mg, 12.5%). <sup>1</sup>H NMR (250 MHz, CDCl<sub>3</sub>): δ 1.25 (s, 9H), 1.55–2.01 (m, 5H), 2.05 (s, 2H), 2.95–3.21 (m, 2H), 3.28 (s, 3H), 3.30–3.82 (m, 3H), 3.85 (s, 3H), 5.00 (s, 2H), 6.65–6.85 (m, 2H), 6.88–7.00

(m, 2H), 7.01–7.20 (m, 2H), 7.50–7.60 (m, 2H), 7.65–7.80 (m, 2H), 8.60–8.75 (s, 2H). <sup>13</sup>C NMR (250 MHz, CDCl<sub>3</sub>): δ 21.45, 28.83, 29.75, 30.09, 41.50, 45.17, 47.76, 49.50, 56.52, 57.41, 60.81, 95.71, 111.07, 112.38, 112.80, 114.69, 121.24, 127.00, 133.07, 143.14, 143.32, 148.48, 148.58, 150.85, 152.50, 156.80. MS (70 eV), *m/z* (%): 637 (100, M<sup>+</sup> + 1).

**(3R,4S)-N-(4-{[4-(2-Fluoro-6-hydroxy-3-methoxy-benzoyl)-phenylamino]-methyl]-azepan-3-yl)-isonicotinamide hydrochloride (6)**. HCl in dioxane (4 M, 1 mL, 4.0 mmol) was added to a solution of **23** (11.5 mg, 0.02 mmol) in 2 mL anhydrous dioxane. The mixture was stirred for 15 h at room temperature, and the volatile components were evaporated. The residue was dissolved in a minimum of MeOH, and anhydrous ether was added to precipitate the product. The resulting light yellow amorphous powder was separated and washed with anhydrous ether (9.4 mg, 95%). <sup>1</sup>H NMR (250 MHz, CD<sub>3</sub>OD): δ 1.45–2.50 (m, 5H), 3.05–3.85 (m, 7H), 4.05 (s, 3H), 6.65–6.95 (m, 4H), 7.20–7.80 (m, 2H), 7.90–8.30 (m, 2H), 8.70–9.0 (m, 2H). <sup>13</sup>C NMR (250 MHz, CD<sub>3</sub>OD): δ 24.73, 29.41, 30.19, 43.43, 44.32, 60.83, 63.55, 73.06, 111.55, 114.50, 117.88, 128.67, 128.85, 129.55, 130.37, 134.10, 134.24, 137.55, 146.46, 151.55, 152.50, 164.00, 164.50. MS (70 eV), *m/z* (%): 493 (100, M<sup>+</sup> + 1); HR-MS (ESI): calcd for C<sub>27</sub>H<sub>30</sub>N<sub>4</sub>O<sub>4</sub>F [M + H]: 493.2251; found: 493.2233.

**4-{[(2-Fluoro-3-methoxy-6-methoxymethoxyphenyl)-(1,1,1-triisopropylsilyloxy)-methyl]-benzoic Acid Methyl Ester (25)**. Carbinol **24**<sup>34</sup> (500 mg, 1.43 mmol), imidazole (244 mg, 3.58 mmol), TIPS-Cl (359 mg, 1.86 mmol) in anhydrous DMF were stirred for 15 h at room temperature. TIPSOSO<sub>2</sub>CF<sub>3</sub> (0.7 equiv) was added, and the mixture was stirred for 36 h at 100 °C. Water (5 mL) was added, and the suspension was extracted with ethyl acetate (3 × 10 mL). The combined organic layers were washed with brine and dried over Na<sub>2</sub>SO<sub>4</sub>. After filtration and evaporation, the residue was purified by flash chromatography on silica gel (column, 2 cm × 15 cm; eluent, (1) ethyl acetate/heptane = 1:9). A colorless oil was obtained (650 mg, 90%). <sup>1</sup>H NMR (250 MHz, CDCl<sub>3</sub>):

$\delta$  0.85–1.19 (m, 18H), 3.32 (s, 3H), 3.72 (s, 3H), 3.79 (s, 3H), 4.98–5.08 (m, 2H), 6.42 (s, 1H), 6.67–6.78 (m, 2H), 7.50 (d,  $^3J = 8.3$  Hz, 2H), 7.87 (d,  $^3J = 8.3$  Hz, 2H).  $^{13}\text{C}$  NMR (62.5 MHz,  $\text{CDCl}_3$ ):  $\delta$  12.67, 18.17, 52.34, 56.37, 57.21, 67.96, 95.61, 109.52, 113.26, 123.00, 125.69, 128.68, 129.54, 143.45, 149.00, 149.998, 151.40 (d,  $^2J = 250$  Hz), 167.58. MS (70 eV),  $m/z$  (%): 507 (100,  $\text{M}^+ + 1$ ).

**{4-[(2-Fluoro-3-methoxy-6-methoxymethoxy-phenyl)-(1,1,1-triisopropylsilyloxy)-methyl]-phenyl}-methanol (26)**. Compound **25** (650 mg, 1.28 mmol) was dissolved in anhydrous THF (8 mL).  $\text{LiAlH}_4$  (106 mg, 2.80 mmol) was added portionwise, and the mixture was stirred for 3 h at room temperature. Water (5 mL) was added, and the suspension was extracted with ethyl acetate ( $3 \times 10$  mL). The combined organic layers were washed with brine and dried over  $\text{Na}_2\text{SO}_4$ . After filtration and evaporation, the residue was purified by flash chromatography on silica gel (column, 2 cm  $\times$  15 cm; eluent, (1) ethyl acetate/heptane = 1:3). A colorless oil was obtained (430 mg, 70%).  $^1\text{H}$  NMR (250 MHz,  $\text{CDCl}_3$ ):  $\delta$  0.97–1.22 (m, 18H), 3.51 (s, 3H), 3.86 (s, 3H), 4.70 (s, 2H), 5.19 (s, 2H), 6.53 (s, 1H), 6.78–6.90 (m, 2H), 7.35 (d,  $^3J = 8.3$  Hz, 2H), 7.57 (d,  $^3J = 8.3$  Hz, 2H).  $^{13}\text{C}$  NMR (250 MHz,  $\text{CDCl}_3$ ):  $\delta$  12.68, 18.22, 56.38, 57.19, 65.75, 68.08, 95.70, 109.52, 112.98, 123.70, 126.18, 126.96, 139.30, 143.63, 144.31, 149.04, 153.10. MS (70 eV),  $m/z$  (%): 479 (100,  $\text{M}^+ + 1$ ).

**[(4-Chloromethyl-phenyl)-(2-fluoro-3-methoxy-6-methoxymethoxy-phenyl)-methoxy]-(1,1,1-triisopropyl)-silane (27)**. Compound **26** (210 mg, 0.44 mmol) and  $\text{PPH}_3$  (115 mg, 0.44 mmol) were dissolved in anhydrous  $\text{CCl}_4$  (5 mL). The mixture was stirred for 3 h at room temperature. Water (5 mL) was added, and the suspension was extracted with ethyl acetate ( $3 \times 10$  mL). The combined organic layers were washed with brine and dried over  $\text{Na}_2\text{SO}_4$ . After filtration and evaporation, the residue was purified by flash chromatography on silica gel (column, 2 cm  $\times$  10 cm; eluent, (1) ethyl acetate/heptane = 1:9) to yield a colorless oil (162 mg, 74%).  $^1\text{H}$  NMR (250 MHz,  $\text{CDCl}_3$ ):  $\delta$  0.85–1.19 (m, 18H), 3.32 (s, 3H), 3.70 (s, 3H), 4.48 (s, 2H), 5.04 (q,  $^3J = 5.6$  Hz, 2H), 6.39 (s, 1H), 6.63–6.78 (m, 2H), 7.20 (d,  $^3J = 8.3$  Hz, 2H), 7.43 (d,  $^3J = 8.3$  Hz, 2H).  $^{13}\text{C}$  NMR (250 MHz,  $\text{CDCl}_3$ ):  $\delta$  12.56, 18.20, 56.36, 57.18, 67.08, 67.96, 95.51, 109.35, 113.02, 123.35, 126.34, 128.88, 132.57, 136.09, 143.37, 145.14, 148.94. MS (70 eV),  $m/z$  (%): 498 (100,  $\text{M}^+ + 1$ ).

**(3R,4R)-4-[4-[(2-Fluoro-3-methoxy-6-methoxymethoxy-phenyl)-(1,1,1-triisopropylsilyloxy)-methyl]-benzyloxy]-azepane-1-carboxylic Acid *tert*-Butyl Ester (28)**.  $\text{NaH}$  (8.0 mg, 0.3 mmol) was added to a solution of (3R,4S)-3-amino-4-hydroxy-azepane-1-carboxylic acid *tert*-butyl ester **28<sup>48</sup>** (83 mg, 0.36 mmol) in anhydrous THF (2 mL). The mixture was stirred for 30 min at reflux, a solution of **27** (160 mg, 0.32 mmol) in anhydrous THF (1 mL) was added and stirring was continued for 2 h at reflux. Water (5 mL) was added, and the suspension was extracted with ethyl acetate ( $3 \times 10$  mL). The combined organic layers were washed with brine and dried over  $\text{Na}_2\text{SO}_4$ . After filtration and evaporation, the residue was purified by flash chromatography on silica gel (column, 2 cm  $\times$  10 cm; eluent, ethyl acetate/2N  $\text{NH}_3$  in MeOH = 98:2) to yield a colorless oil (102 mg, 43%).  $^1\text{H}$  NMR (250 MHz,  $\text{CDCl}_3$ ):  $\delta$  0.85 (s, 18H), 1.35 (s, 9H), 1.40–1.55 (m, 4H), 2.75–3.20 (m, 4H), 3.35 (s, 3H), 3.35–3.57 (m, 2H), 3.67 (s, 3H), 4.21–4.58 (m, 2H), 5.01–5.09 (m, 2H), 6.39 (s, 1H), 6.62–6.78 (m, 2H), 7.11–7.23 (m, 2H), 7.39–7.48 (m, 2H).  $^{13}\text{C}$  NMR (250 MHz,  $\text{CDCl}_3$ ):  $\delta$  12.28, 17.84, 22.52, 27.31, 28.83, 46.00, 47.11, 47.63, 56.53, 57.16, 68.09, 71.35, 79.98, 84.88, 95.68, 109.39, 112.91, 123.67, 126.04, 127.57, 136.72, 143.43, 144.21, 148.91, 156.04, 175.14. MS (70 eV),  $m/z$  (%): 692 (100,  $\text{M}^+ + 1$ ).

**(3R,4R)-4-[4-[(1,1,1-Triisopropylsilyloxy)-(2-fluoro-3-methoxy-6-methoxymethoxy-phenyl)-methyl]-benzyloxy]-3-[(pyridine-4-carbonyl)-amino]-azepane-1-carboxylic Acid *tert*-Butyl Ester (29)**. Compound **28** (102 mg, 0.15 mmol) was dissolved in anhydrous  $\text{CH}_2\text{Cl}_2$  (2 mL). Isonicotinic acid (21 mg, 0.17 mmol), DMAP (10 mg, 0.1 mmol), and DCC (36 mg, 0.17 mmol) were added to this solution, and the mixture was stirred for 15 h. Water (5 mL) was added, and

the suspension was extracted with  $\text{CH}_2\text{Cl}_2$  ( $3 \times 10$  mL). The combined organic layers were washed with brine and dried over  $\text{Na}_2\text{SO}_4$ . After filtration and evaporation, a colorless oil was obtained (114 mg, 92%).  $^1\text{H}$  NMR (250 MHz,  $\text{CDCl}_3$ ):  $\delta$  0.85–1.05 (m, 18H), 1.41 (s, 9H), 1.48–2.02 (m, 4H), 2.91–3.05 (m, 1H), 3.15–3.29 (m, 1H), 3.36 (s, 3H), 3.70 (s, 3H), 3.90–4.07 (m, 3H), 4.18–4.25 (m, 1H), 4.52–4.60 (s, 2H), 5.00–5.10 (m, 2H), 6.38 (s, 1H), 6.62–6.78 (m, 2H), 7.19 (d,  $^3J = 8.3$  Hz, 2H), 7.37 (d,  $^3J = 8.3$  Hz, 2H), 7.62 (br d, 2H), 8.29 (br s, 1H), 8.57–8.69 (m, 2H). MS (70 eV),  $m/z$  (%): 797 (100,  $\text{M}^+ + 1$ ).

**(3R,4R)-4-[4-(2-Fluoro-3-methoxy-6-methoxymethoxy-benzyloxy)-3-[(pyridine-4-carbonyl)-amino]-azepane-1-carboxylic Acid *tert*-Butyl Ester (30)**. Compound **29** (114 mg, 0.14 mmol) and  $\text{Bu}_4\text{NF} \cdot 4 \text{H}_2\text{O}$  (183 mg, 0.70 mmol) in THF (2 mL) were stirred for 15 h at room temperature. Water (5 mL) was added, and the suspension was extracted with ethyl acetate ( $3 \times 10$  mL). The combined organic layers were washed with brine and dried over  $\text{Na}_2\text{SO}_4$ . After filtration and evaporation, the residue was purified by flash chromatography on silica gel (column, 2 cm  $\times$  10 cm; eluent, (1) ethyl acetate) to yield a colorless crude oil (70 mg, 76%) which was dissolved in anhydrous  $\text{CH}_2\text{Cl}_2$  (2 mL). Activated  $\text{MnO}_2$  (50 mg) was added, and the mixture was stirred for 24 h. After filtration through a plug of Celite and evaporation, the residue was purified by flash chromatography on silica gel (column, 2 cm  $\times$  10 cm; eluent, ethyl acetate) to yield a colorless crude oil (50 mg, 72%).  $^1\text{H}$  NMR (250 MHz,  $\text{CDCl}_3$ ):  $\delta$  1.48 (s, 9H), 1.52–2.08 (m, 4H), 2.97–3.09 (1H), 3.24–3.36 (m, 1H), 3.27 (s, 3H), 3.72–3.82 (m, 1H), 3.86 (s, 3H), 4.02–4.13 (m, 2H), 4.74 (s, 2H), 4.99 (s, 2H), 6.89–7.0 (m, 2H), 7.43 (d,  $^3J = 9.1$  Hz, 2H), 7.67 (d,  $^3J = 6.8$  Hz, 2H), 7.83 (d,  $^3J = 9.1$  Hz, 2H), 8.43 (br d, 1H), 8.72 (d,  $^3J = 6.8$  Hz, 2H).  $^{13}\text{C}$  NMR (250 MHz,  $\text{CDCl}_3$ ):  $\delta$  21.19, 25.27, 28.77, 33.42, 47.19, 47.93, 55.21, 56.56, 57.42, 70.92, 81.27, 95.66, 110.99, 115.26, 121.29, 127.56, 130.18, 136.64, 141.60, 143.15, 145.39, 148.55, 149.63, 150.93, 159.06, 165.45, 191.39. MS (70 eV),  $m/z$  (%): 638 (100,  $\text{M}^+ + 1$ ).

**(3R,4R)-N-{4-[4-(2-Fluoro-6-hydroxy-3-methoxy-benzyloxy)-azepan-3-yl]-isonicotinamide hydrochloride (5)}**.  $\text{HCl}$  in dioxane (4 M, 2 mL, 8.0 mmol) was added to a solution of **30** (45.0 mg, 0.07 mmol) in anhydrous MeOH (2 mL). The mixture was stirred for 15 h at room temperature, and the volatile components were evaporated. The residue was dissolved in a minimum of MeOH, and anhydrous diethyl ether was added to precipitate the product. The resulting light yellow amorphous powder was separated and washed with anhydrous diethyl ether (40 mg, 91%).  $^1\text{H}$  NMR (250 MHz,  $\text{D}_2\text{O}$ ):  $\delta$  1.89–2.38 (m, 3H), 2.32–2.35 (m, 1H), 3.27–3.48 (m, 3H), 3.85–3.92 (m, 2H), 3.92 (s, 3H), 4.24–4.32 (m, 1H), 4.53 (d,  $^3J = 14.1$  Hz, 1H), 4.83 (d,  $^3J = 14.1$  Hz, 1H), 6.83 (d,  $^3J = 9.1$  Hz, 1H), 7.27 (d,  $^3J = 9.1$  Hz, 1H), 7.42 (d,  $^3J = 8.3$  Hz, 2H), 7.60 (d,  $^3J = 8.3$  Hz, 2H), 7.96 (d,  $^3J = 6.7$  Hz, 2H), 8.85 (d,  $^3J = 6.7$  Hz, 2H).  $^{13}\text{C}$  NMR (62.5 MHz,  $\text{D}_2\text{O}$ ):  $\delta$  19.30, 27.59, 45.79, 47.20, 52.82, 57.02, 69.99, 79.55, 111.55, 117.56, 124.16, 124.23, 128.93, 129.00, 129.74, 135.59, 140.03, 140.85, 143.35, 144.40, 147.06, 164.13, 194.54. MS (70 eV),  $m/z$  (%): 567 (100,  $\text{M}^+ + 1$ ); HR-MS (ESI): calcd for  $\text{C}_{27}\text{H}_{29}\text{N}_3\text{O}_5\text{F}$  [ $\text{M} + \text{H}$ ]: 494.2091; found: 494.2101.

**(2-Fluoro-3-methoxy-6-methoxymethoxy-phenyl)-(4-hydroxymethyl-phenyl)-methanol (31)**. A suspension of  $\text{LiAlH}_4$  (0.68 g, 17.8 mmol) in anhydrous THF (10 mL) was added during 15 min to a solution of 4-[(2-fluoro-3-methoxy-6-methoxymethoxy-phenyl)-hydroxy-methyl]-benzoic acid methyl ester **24** (3.0 g, 8.9 mmol) in anhydrous THF (25 mL) at room temperature. The mixture was stirred for 3 h at room temperature. Water (5 mL) was added dropwise at  $0^\circ\text{C}$ . After stirring for 30 min water (15 mL) was added and the mixture was filtered. The filter cake was washed with ethyl acetate ( $3 \times 4$  mL) and the aqueous layer re-extracted with ethyl acetate ( $2 \times 10$  mL). The combined organic layers were washed with brine ( $2 \times 3$  mL), dried over  $\text{Na}_2\text{SO}_4$ , filtered, and concentrated in vacuo to yield a colorless viscous oil (1.8 g, 63%).  $^1\text{H}$  NMR (500 MHz,  $\text{CDCl}_3$ ):  $\delta$  1.70 (br, 2H), 3.28 (s, 3H), 3.87 (s, 3H),

4.67 (s, 2H), 4.98 (d, 1H), 5.06 (d, 1H), 6.25 (s, 1H), 6.82–6.87 (m, 2H), 7.31 (d, 2H), 7.37 (d, 2H);  $^{13}\text{C}$  NMR (100 MHz,  $\text{CDCl}_3$ ):  $\delta$  56.22, 56.82, 65.11, 68.18, 95.08, 109.97, 112.67, 121.38, 125.72, 126.86, 139.66, 142.92, 143.08, 148.85, 148.91. HR-MS (EI): calcd for  $\text{C}_{17}\text{H}_{19}\text{O}_5\text{F}^+$  [ $\text{M}^+$ ]: 322.1211; found: 322.1223.

**4-(2-Fluoro-3-methoxy-6-methoxymethoxy-benzoyl)-benzaldehyde (32).** Activated  $\text{MnO}_2$  (0.78 g, 9.00 mmol) was added to a solution of **31** (1.8 g, 5.6 mmol) in  $\text{CH}_2\text{Cl}_2$  (150 mL). Two further portions of activated  $\text{MnO}_2$  ( $2 \times 0.78$  g, 9.00 mmol) were added after 2 and 4 h of vigorous stirring. The stirring was continued for 15 h. The filter cake was washed with  $\text{CH}_2\text{Cl}_2$  ( $3 \times 30$  mL), and the combined organic layers were concentrated in vacuo to yield light yellow crystals (1.22 g, 69%, mp. 104–106 °C).  $^1\text{H}$  NMR (500 MHz,  $\text{CDCl}_3$ ):  $\delta$  3.31 (s, 3H), 3.92 (s, 3H), 5.03 (s, 2H), 6.98 (d, 1H), 7.05 (t, 1H), 7.99 (d, 2H), 8.04 (d, 2H), 10.14 (s, 1H);  $^{13}\text{C}$  NMR (100 MHz,  $\text{CDCl}_3$ ):  $\delta$  56.24, 57.09, 95.33, 110.69, 115.59, 119.11, 129.77, 130.00, 139.43, 141.26, 143.02, 148.30, 150.59, 190.76, 191.60. HR-MS (EI): calcd for  $\text{C}_{17}\text{H}_{15}\text{O}_5\text{F}^+$  [ $\text{M}^+$ ]: 318.0898; found: 318.0903.

**(3R,4R)-4-[4-(2-Fluoro-3-methoxy-6-methoxymethoxy-benzoyl)-benzylidene]-amino-3-[(pyridine-4-carbonyl)-amino]-azepane-1-carboxylic Acid *tert*-Butyl Ester (33).** Compound **32** (0.78 g, 9.00 mmol) was added to a solution of amine **14** (1.8 g, 5.6 mmol) in  $\text{C}_2\text{H}_5\text{OH}$  (150 mL). The solution was heated at reflux under argon for 15 h and stirred for 48 h at room temperature. The volatile components were evaporated to yield an off-white foam (302 mg, 95%).  $^1\text{H}$  NMR (500 MHz,  $\text{CDCl}_3$ ):  $\delta$  1.57 (s, 9H), 1.83–1.99 (m, 4H), 3.20 (d, 1H), 3.31 (s, 3H), 3.54 (d, 1H), 3.90 (s, 3H), 3.96 (d, 1H), 3.97 (m, 1H), 4.13 (m, 1H), 4.16 (d, 1H), 5.02 (s, 2H), 6.95 (t, 1H), 7.02 (t, 1H), 7.70 (s, 2H), 7.83 (d, 2H), 7.92 (d, 2H), 8.47 (s, 1H), 8.57 (s, 1H), 8.74 (s, 2H).  $^{13}\text{C}$  NMR (100 MHz,  $\text{CDCl}_3$ ):  $\delta$  22.92, 28.07, 28.46, 48.43, 48.90, 56.22, 57.10, 58.67, 61.23, 70.46, 80.75, 95.34, 110.68, 115.24, 115.56, 120.94, 128.40, 129.87, 138.58, 140.67, 141.26, 142.88, 148.29, 149.66, 150.53, 165.89, 190.96, 191.61.

**(3R,4R)-4-[4-(2-Fluoro-3-methoxy-6-methoxymethoxy-benzoyl)-benzylamino]-3-[(pyridine-4-carbonyl)-amino]-azepane-1-carboxylic Acid *tert*-Butyl Ester (34).**  $\text{NaBH}_3\text{CN}$  (35.0 mg, 0.56 mmol) was added to a solution of **14** (180 mg, 0.28 mmol) in  $\text{CH}_3\text{OH}$  (3 mL), and the resulting mixture was stirred for 1 h at room temperature. Water (25 mL) was added, and the suspension was extracted with ethyl acetate ( $3 \times 20$  mL). The combined organic layers were washed with brine and dried over  $\text{Na}_2\text{SO}_4$ . After filtration and evaporation, the residue was purified by flash chromatography on silica gel (column, 2 cm  $\times$  15 cm; eluent, (1) ethyl acetate/heptane, (2) ethyl acetate to (3) ethyl acetate/ $\text{CH}_3\text{OH}$  = 95:5). A yellow gum was obtained as raw material (102 mg, 57%). HR-MS (ESI): calcd for  $\text{C}_{34}\text{H}_{42}\text{N}_4\text{O}_7\text{F}$  [ $\text{M} + \text{H}$ ]: 637.3038; found: 637.3082.

**(3R,4R)-N-[4-[4-(2-Fluoro-6-hydroxy-3-methoxy-benzoyl)-benzylamino]-azepane-3-yl]-isonicotinamide Hydrochloride (7).** HCl in dioxane (4 M, 3 mL, 12.0 mmol) was added to a solution of **34** (45.0 mg, 0.07 mmol) in anhydrous dioxane (2 mL). The mixture was stirred for 15 h at room temperature, and the resulting light yellow crystals were separated and washed with anhydrous diethyl ether (24 mg, 57%, mp 196 °C dec).  $^1\text{H}$  NMR (500 MHz, DMSO):  $\delta$  1.93 (m, 1H), 2.08 (m, 1H), 2.19 (m, 1H), 2.35 (m, 1H), 3.05 (m, 1H), 3.25 (m, 1H), 3.40 (s, 2H), 3.79 (s, 3H), 4.25 (m, 1H), 4.37 (m, 1H), 4.92 (m, 1H), 6.76 (d, 1H), 7.15 (t, 1H), 7.72 (d, 2H), 7.75 (d, 2H), 7.97 (d, 2H), 8.77 (d, 2H), 9.61–10.01 (m, 5H).  $^{13}\text{C}$  NMR (100 MHz, DMSO):  $\delta$  22.5, 25.7, 46.9, 47.0, 48.0, 48.3, 57.3, 61.2, 111.3, 116.4, 116.8, 122.5, 129.5, 131.2, 136.9, 138.3, 140.3, 141.5, 149.6, 149.8, 151.0, 165.4, 191.7. HR-MS (ESI): calcd for  $\text{C}_{27}\text{H}_{30}\text{N}_4\text{O}_4\text{F}$  [ $\text{M} + \text{H}$ ]: 493.2251; found: 493.2250.

**(3R)-4-Oxo-3-[(pyridine-4-carbonyl)-amino]-azepane-1-carboxylic Acid *tert*-Butyl Ester (35).** Oxalyl chloride (1.07 mL, 12.3 mmol) was dissolved in anhydrous  $\text{CH}_2\text{Cl}_2$  (25 mL) and cooled to  $-78$  °C. DMSO (1.93 g, 24.7 mmol) in  $\text{CH}_2\text{Cl}_2$  (3 mL) was added to this solution at  $-78$  °C, and the mixture was stirred for 5 min. Compound **11** (3.76 g, 11.2

mmol) in  $\text{CH}_2\text{Cl}_2$  (10 mL) was added during 5 min at  $-78$  °C, and the mixture was stirred for 20 min at this temperature. Triethylamine (8.3 mL, 60 mmol) was added, and the mixture was stirred for 5 min and slowly warmed to room temperature. Water (5 mL) was added, and the suspension was extracted with  $\text{CH}_2\text{Cl}_2$  ( $3 \times 10$  mL). The combined organic layers were washed with brine and dried over  $\text{Na}_2\text{SO}_4$ . After filtration and evaporation, the residue was purified by flash chromatography on silica gel (column, 4 cm  $\times$  25 cm; eluent, ethyl acetate/ $\text{MeOH}$ -2N  $\text{NH}_3$  = 95:5) to yield a light yellow gum (3.18 g, 85%).  $^1\text{H}$  NMR (250 MHz,  $\text{CDCl}_3$ ):  $\delta$  1.38 (s, 2H), 1.44 (s, 7H), 1.65–2.09 (m, 2H), 2.55–2.90 (m, 2H), 2.92–3.05 (m, 0.75H), 3.18–3.40 (0.25H), 3.60–4.25 (m, 3H), 4.85–4.96 (m, 0.25H), 4.96–5.14 (m, 0.75H), 7.72 (d,  $^3J$  = 5.4 Hz, 2H), 8.20 (br d, 1H), 8.88 (d,  $^3J$  = 5.4 Hz, 2H).  $^{13}\text{C}$  NMR (62.5 MHz,  $\text{CDCl}_3$ ):  $\delta$  two rotamers: A: 27.29, 28.61, 40.03, 49.28, 51.09, 62.21, 81.61, 121.46, 141.42, 150.90, 156.81, 165.43, 206.36; B: 25.13, 28.62, 40.15, 48.67, 48.88, 61.03, 81.08, 121.29, 141.00, 150.90, 155.11, 165.06, 207.36. MS (70 eV),  $m/z$  (%): 334 (100,  $\text{M}^+ + 1$ ); HR-MS (ESI): calcd for  $\text{C}_{17}\text{H}_{23}\text{N}_3\text{O}_4$  [ $\text{M} + \text{H}$ ]: 334.1767; found: 334.1782.

**(3R)-4-Methoxymethylene-3-[(pyridine-4-carbonyl)-amino]-azepane-1-carboxylic Acid *tert*-Butyl Ester (36).** Potassium *tert*-butoxide (1.60 g, 13.9 mmol) was added over a period of 0.5 h via a sidearm addition funnel under argon atmosphere to a suspension of (methoxymethyl)-triphenylphosphonium chloride (4.90 g, 13.9 mmol) in anhydrous diethyl ether (60 mL) at  $-15$  °C. The reaction mixture was stirred at  $-15$  °C for 1 h, and then a solution of ketone **35** (1.65 g, 4.95 mmol) in anhydrous diethyl ether (20 mL) was added over a period of 20 min at this temperature. Stirring at room temperature was continued for 24 h. The reaction mixture was hydrolyzed with water (30 mL), and the organic and aqueous phases were separated. The aqueous phase was re-extracted with diethyl ether ( $2 \times 20$  mL), and the combined organic layers were dried over  $\text{Na}_2\text{SO}_4$ . Cooling of the organic phase to  $-30$  °C resulted in crystallization of triphenylphosphine oxide, which was separated by decantation. After filtration and evaporation, the residue was purified by flash chromatography on silica gel (column, 4 cm  $\times$  25 cm; eluent, ethyl acetate/ $\text{MeOH}$ -2 N  $\text{NH}_3$  = 99:1) to yield a light yellow gum (1.05 g, 59%).  $^1\text{H}$  NMR (400 MHz,  $\text{CDCl}_3$ ):  $\delta$  1.45 (s, 2H), 1.51 (s, 7H), 1.62–2.19 (m, 4H), 2.82–2.96 (m, 2H), 3.55–3.70 (m, 3H), 3.80–3.91 (m, 1H), 4.18–4.30 (m, 1H), 5.20 (br s, 1H), 6.00 (s, 1H), 7.66 (d,  $^3J$  = 5.2 Hz, 2H), 8.20 (br d, 1H), 8.70 (d,  $^3J$  = 5.2 Hz, 2H).  $^{13}\text{C}$  NMR (62.5 MHz,  $\text{CDCl}_3$ ):  $\delta$  21.05, 28.41, 47.63, 50.29, 52.53, 60.10, 71.12, 80.44, 114.07, 120.91, 131.74, 145.75, 150.47, 157.99, 164.33. MS (70 eV),  $m/z$  (%): 362 (100,  $\text{M}^+ + 1$ ); HR-MS (ESI): calcd for  $\text{C}_{19}\text{H}_{28}\text{N}_3\text{O}_4$  [ $\text{M} + \text{H}$ ]: 362.2080; found: 362.2071.

**(3R,4S)-4-Formyl-3-[(pyridine-4-carbonyl)-amino]-azepane-1-carboxylic Acid *tert*-Butyl Ester (37).** Enol ether **36** (200 mg, 0.55 mmol) was stirred in  $\text{CHCl}_3$  (30 mL) at reflux. Trichloroacetic acid (200 mg, 2.77 mmol) was added via a sidearm addition funnel. The mixture was stirred for 60 min at reflux and then cooled to room temperature. The reaction mixture was washed with saturated aqueous  $\text{NaHCO}_3$  solution (10 mL), and after separation the aqueous phase was re-extracted with  $\text{CH}_2\text{Cl}_2$  ( $2 \times 5$  mL). The combined organic layers were washed with brine and dried over  $\text{Na}_2\text{SO}_4$ . After filtration and evaporation the residue was purified by flash chromatography on silica gel (column, 4 cm  $\times$  25 cm; eluent, ethyl acetate/ $\text{MeOH}$ -2 N  $\text{NH}_3$  = 99:1) to yield a light yellow oil (130 mg, 68%). The product contains 20% (3R,4S)-4-formyl-3-[(pyridine-4-carbonyl)-amino]-azepane-1-carboxylic acid *tert*-butyl ester.  $^1\text{H}$  NMR (400 MHz,  $\text{CDCl}_3$ ):  $\delta$  1.53 (s, 9H), 1.51–2.19 (m, 4H), 2.55–2.94 (m, 2H), 3.14–3.24 (m, 1H), 3.82–4.25 (m, 2H), 4.18–4.30 (m, 1H), 4.51–4.84 (m, 1H), 7.57–7.78 (m, 2H), 8.70–8.85 (m, 2H), 9.81 (s, 1H). MS (70 eV),  $m/z$  (%): 348 (100,  $\text{M}^+ + 1$ ); HR-MS (ESI): calcd for  $\text{C}_{18}\text{H}_{26}\text{N}_3\text{O}_4$  [ $\text{M} + \text{H}$ ]: 348.1923; found: 364.1889.

**(3R,4S)-3-[(Pyridine-4-carbonyl)-amino]-4-vinyl-azepane-1-carboxylic Acid *tert*-Butyl Ester (38).** *n*-BuLi solution (1.6 M in hexane, 605  $\mu\text{L}$ , 0.97 mmol) was added to a

suspension of methyltriphenylphosphonium iodide (390 mg, 0.97 mmol) in anhydrous THF (10 mL). The mixture was stirred for 40 min at  $-10^{\circ}\text{C}$  and then cooled to  $-78^{\circ}\text{C}$ . Aldehyde **37** (240 mg, 0.69 mmol) in THF (5 mL) was added, and the mixture was warmed to room temperature in a period of 14 h. Water (5 mL) and ethyl acetate (5 mL) were added, and the separated aqueous layer was re-extracted with ethyl acetate ( $2 \times 5$  mL). The combined organic layers were washed with brine and dried over  $\text{Na}_2\text{SO}_4$ . After filtration and evaporation, the residue was purified by preparative HPLC (Chiracel OD CSP 20  $\mu\text{m}$  from Daicel, 2-propanol/heptane = 1:4 as eluent) to yield a light yellow oil (120 mg, 50%).  $^1\text{H}$  NMR (400 MHz,  $\text{CDCl}_3$ ):  $\delta$  1.53 (s, 9H), 1.51–1.78 (m, 4H), 2.10–2.19 (m, 1H), 2.72–2.83 (m, 1H), 3.29 (dd,  $^3J = 15.3$  Hz, 5.6 Hz, 1H), 3.92–4.05 (m, 2H), 4.21–4.32 (m, 1H), 4.93–5.08 (m, 2H), 5.80–5.94 (m, 1H), 7.50 (m, 2H), 8.21 (d,  $^3J = 7.3$  Hz, 1H), 8.73 (d,  $^3J = 4.2$  Hz, 2H).  $^{13}\text{C}$  NMR (100 MHz,  $\text{CDCl}_3$ ):  $\delta$  27.02, 27.41, 28.16, 48.02, 49.18, 51.27, 53.65, 79.76, 113.68, 119.94, 139.53, 140.89, 149.46, 157.21, 163.15. MS (70 eV),  $m/z$  (%): 346 (100,  $\text{M}^+ + 1$ ); HR-MS (ESI): calcd for  $\text{C}_{19}\text{H}_{28}\text{N}_3\text{O}_3$  [ $\text{M} + \text{H}$ ]: 346.2131; found: 346.2131.

**(3R,4S)-4-[(trans-2-[4-(2-Fluoro-3-methoxy-6-methoxy-methoxy-benzoyl)-phenyl]-vinyl)-3-[(pyridine-4-carboxyl)-amino]-azepane-1-carboxylic Acid tert-Butyl Ester (39)**. Alkene **38** (60 mg, 0.17 mmol), iodide **19** (65 mg, 0.16 mmol), Pd(II) acetate (3.90 mg, 0.017 mmol), tri-*o*-tolylphosphine (10.9 mg, 0.034 mmol), and *N,N*-diisopropylamine (60.1  $\mu\text{L}$ , 0.34 mmol) were dissolved in anhydrous DMF (1 mL) and stirred for 14 h at  $105^{\circ}\text{C}$ . The volatile components were evaporated in vacuo and the residue was purified by flash chromatography on silica gel (column, 1.5 cm  $\times$  15 cm; eluent, ethyl acetate/MeOH = 19:1) to yield a dense colorless oil (20 mg, 18%).  $^1\text{H}$  NMR (400 MHz,  $\text{CDCl}_3$ ):  $\delta$  1.54 (s, 9H), 1.51–1.92 (m, 4H), 2.33–2.42 (m, 1H), 2.72–2.88 (m, 1H), 3.25–3.39 (m, 1H), 3.29 (s, 3H), 3.87 (s, 3H), 3.95–4.09 (m, 2H), 4.32–4.42 (m, 1H), 5.00 (s, 2H), 6.32–6.45 (m, 2H), 6.87–7.02 (m, 2H), 7.35 (d,  $^3J = 8.3$  Hz, 2H), 7.58 (d,  $^3J = 5.3$  Hz, 2H), 7.77 (d,  $^3J = 8.2$  Hz, 2H), 8.28 (d,  $^3J = 7.8$  Hz, 1H), 8.68 (d,  $^3J = 5.4$  Hz, 2H). MS (70 eV),  $m/z$  (%): 634 (100,  $\text{M}^+ + 1$ ).

**(3R,4S)-N-(4-[(trans-2-[4-(2-Fluoro-6-hydroxy-3-methoxy-benzoyl)-phenyl]-vinyl)-azepan-3-yl]-isonicotinamide Hydrochloride (8)**. HCl in diethyl ether (2 M, 180  $\mu\text{L}$ , 0.36 mmol) was added to a solution of **39** (8.00 mg, 0.0126 mmol) in anhydrous MeOH (0.2 mL) and anhydrous diethyl ether (0.5 mL). The mixture was stirred for 15 h at room temperature, and the volatile components were evaporated. The residue was dissolved in a minimum of MeOH, and anhydrous diethyl ether was added to precipitate the product. The resulting light yellow amorphous powder was separated and washed with anhydrous diethyl ether (7 mg, 98%).  $^1\text{H}$  NMR (500 MHz,  $\text{CD}_3\text{OD}$ ):  $\delta$  1.82–2.20 (m, 4H), 2.86–2.96 (m, 1H), 3.12–3.75 (m, 4H), 3.84 (s, 3H), 4.39 (br s, 1H), 6.38–6.48 (m, 1H), 6.58–6.76 (m, 3H), 7.06–7.17 (m, 2H), 7.47 (d,  $^3J = 8.0$  Hz, 2H), 7.73 (d,  $^3J = 7.8$  Hz, 2H), 8.36 (br s, 8.36, 2H), 8.97 (br s, 2H). MS (70 eV),  $m/z$  (%): 563 (100,  $\text{M}^+ + 1$ ); HR-MS (ESI): calcd for  $\text{C}_{28}\text{H}_{29}\text{N}_3\text{O}_4\text{F}$  [ $\text{M} + \text{H}$ ]: 490.2142; found: 490.2165.

**Acknowledgment.** We thank Dr. Dirk Bossemeyer for providing the protein material PKA for the in vitro assays and the crystallization experiments and Dr. W. von der Saal and Dr. A. Mertens for encouragement and support. We thank Dr. C. Geletneky for NMR and Dr. G. Drabner for mass spectrometry data. Dr. W. Schäfer is thanked for supportive ideas and discussions of the modeling work. We thank Dr. U. Zutter and Dr. T. Hartung for the supply of the starting material **9**. We thank Prof. Dr. F. Diederich for consulting and helpful discussions of this work.

**Supporting Information Available:** X-ray data collection and refinement statistics. This material is available free of charge via the Internet at <http://pubs.acs.org>.

## References

- Masjost, B. S. R.; Schumacher, R.; Friebe, W.-G. Novel azepane derivatives. PCT Int. Appl. WO03/076429 (Roche Diagnostics GmbH, Germany), 2003.
- Cross, T. G.; Scheel-Toellner, D.; Henriquez, N. V.; Deacon, E.; Salmon, M.; Lord, J. M. Serine/threonine protein kinases and apoptosis. *Exp. Cell Res.* **2000**, *256*, 34–41.
- Kozikowski, A. P.; Sun, H.; Brognard, J.; Dennis, P. A. Novel PI analogues selectively block activation of the pro-survival Serine/Threonine Kinase Akt. *J. Am. Chem. Soc.* **2003**, *125*, 1144–1145.
- Vanhaesebroeck, B.; Alessi, D. R. The PI3K–PDK1 connection: more than just a road to PKB. *Biochem. J.* **2000**, *346 Pt 3*, 561–576.
- Blume-Jensen, P.; Hunter, T. Oncogenic kinase signalling. *Nature* **2001**, *411*, 355–365.
- Kandel, E. S.; Hay, N. The regulation and activities of the multifunctional serine/threonine kinase Akt/PKB. *Exp. Cell Res.* **1999**, *253*, 210–229.
- Datta, S. R.; Brunet, A.; Greenberg, M. E. Cellular survival: a play in three Akts. *Genes Dev.* **1999**, *13*, 2905–2927.
- Vivanco, I.; Sawyers, C. L. The phosphatidylinositol 3-Kinase AKT pathway in human cancer. *Nat. Rev. Cancer* **2002**, *2*, 489–501.
- Testa, J. R.; Bellacosa, A. AKT plays a central role in tumorigenesis. *Proc. Natl. Acad. Sci. U.S.A.* **2001**, *98*, 10983–10985.
- Malik, S. N.; Brattain, M.; Ghosh, P. M.; Troyer, D. A.; Prihoda, T.; Bedolla, R.; Kreisberg, J. I. Immunohistochemical demonstration of phospho-Akt in high Gleason grade prostate cancer. *Clin. Cancer Res.* **2002**, *8*, 1168–1171.
- Thakkar, H.; Chen, X.; Tyan, F.; Gim, S.; Robinson, H.; Lee, C.; Pandey, S. K.; Nwokorie, C.; Onwudiwe, N.; Srivastava, R. K. Pro-survival function of Akt/protein kinase B in prostate cancer cells. Relationship with TRAIL resistance. *J. Biol. Chem.* **2001**, *276*, 38361–38369.
- Stal, O.; Perez-Tenorio, G.; Akerberg, L.; Olsson, B.; Nordenskjöld, B.; Skoog, L.; Rutqvist, L. E. Akt kinases in breast cancer and the results of adjuvant therapy. *Breast Cancer Res.* **2003**, *5*, R37–44.
- Nesterov, A.; Lu, X.; Johnson, M.; Miller, G. J.; Ivashchenko, Y.; Kraft, A. S. Elevated AKT activity protects the prostate cancer cell line LNCaP from TRAIL-induced apoptosis. *J. Biol. Chem.* **2001**, *276*, 10767–10774.
- Pawelczak, C. P.; Charboneau, L.; Bichsel, V. E.; Simone, N. L.; Chen, T.; Gillespie, J. W.; Emmert-Buck, M. R.; Roth, M. J.; Petricoin, I. E.; Liotta, L. A. Reverse phase protein microarrays which capture disease progression show activation of pro-survival pathways at the cancer invasion front. *Oncogene* **2001**, *20*, 1981–1989.
- Beresford, S. A.; Davies, M. A.; Gallicci, G. E.; Donato, N. J. Differential effects of phosphatidylinositol-3/Akt-kinase inhibition on apoptotic sensitization to cytokines in LNCaP and PC-3 prostate cancer cells. *J. Interferon Cytokine Res.* **2001**, *21*, 313–322.
- Kumar, C. C.; Diao, R.; Yin, Z.; Liu, Y.; Samatar, A. A.; Madison, V.; Xiao, L. Expression, purification, characterization and homology modeling of active Akt/PKB, a key enzyme involved in cell survival signaling. *Biochim. Biophys. Acta* **2001**, *1526*, 257–268.
- Yang, J.; Cron, P.; Good, V. M.; Thompson, V.; Hemmings, B. A.; Barford, D. Crystal structure of an activated Akt/protein kinase B ternary complex with GSK-3-peptide and AMP–PNP. *Nat. Struct. Biol.* **2002**, *9*, 940–944.
- Yang, J.; Cron, P.; Thompson, V.; Good, V. M.; Hess, D.; Hemmings, B. A.; Barford, D. Molecular mechanism for the regulation of protein kinase B/Akt by hydrophobic motif phosphorylation. *Mol. Cell* **2002**, *9*, 1227–1240.
- Jirousek, M. R.; Gillig, J. R.; Gonzalez, C. M.; Heath, W. F.; McDonald, J. H., 3rd; Neel, D. A.; Rito, C. J.; Singh, U.; Stramm, L. E.; Melikian-Badalian, A.; Baevsky, M.; Ballas, L. M.; Hall, S. E.; Wimmeroski, L. L.; Faul, M. M. (S)-13-[(dimethylamino)methyl]-10,11,14,15-tetrahydro-4,9:16,21-dimetheno-1H,13H-dibenzo[e,k]pyrrolo[3,4-h][1,4,13]oxadiazacyclohexadecene-1,3-(2H)-dione (LY333531) and related analogues: isozyme selective inhibitors of protein kinase C beta. *J. Med. Chem.* **1996**, *39*, 2664–2671.
- Tenzen, A.; Zingg, D.; Rocha, S.; Hemmings, B.; Fabbro, D.; Glanzmann, C.; Schubiger, P. A.; Bodis, S.; Pruschy, M. The phosphatidylinositol 3'-kinase/Akt survival pathway is a target for the anticancer and radiosensitizing agent PKC412, an inhibitor of protein kinase C. *Cancer Res.* **2001**, *61*, 8203–8210.
- Heath, W. F., Jr.; Jirousek, M. R.; McDonald, J. H., III; Rito, C. J. Preparation of bis(indolyl)maleimide macrocycles as beta-isozyme selective protein kinase C inhibitors. Eur. Pat. Appl. (Lilly, Eli, and Co.) EP657458, 1995; 70 pp.
- Caravatti, G.; Fredenhagen, A. Preparation of N-acyl- and N-hydrocarbylstaurosporines as protein kinase C inhibitors. Eur. Pat. Appl. (Ciba-Geigy A.-G., Switz.) EP296110, 1988; 27 pp.

- (23) Kulanthaivel, P.; Hallock, Y.; Boros, C.; Hamilton, S. M.; Janzen, W. P.; Ballas, L. M.; Loomis, C. R.; Jiang, J. B.; Katz, J. B.; Steiner, J. R.; Clardy, J. Balanol: A Novel and Potent Inhibitor of Protein Kinase C from the Fungus *Verticillium balanoides*. *J. Am. Chem. Soc.* **1993**, *115*, 6452–6453.
- (24) Ohshima, S.; Yanagisawa, M.; Katoh, A.; Fujii, T.; Sano, T.; Matsukuma, S.; Furumai, T.; Fujii, M.; Watanabe, K.; Yokose, K.; et al. Fusarium merismoides Corda NR 6356, the source of the protein kinase C inhibitor, azepinostatin. Taxonomy, yield improvement, fermentation and biological activity. *J. Antibiot. (Tokyo)* **1994**, *47*, 639–647.
- (25) Narayana, N.; Diller, T. C.; Koide, K.; Bunnage, M. E.; Nicolaou, K. C.; Brunton, L. L.; Xuong, N. H.; Ten Eyck, L. F.; Taylor, S. S. Crystal structure of the potent natural product inhibitor balanol in complex with the catalytic subunit of cAMP-dependent protein kinase. *Biochemistry* **1999**, *38*, 2367–2376.
- (26) Hunenberger, P. H.; Helms, V.; Narayana, N.; Taylor, S. S.; McCammon, J. A. Determinants of ligand binding to cAMP-dependent protein kinase. *Biochemistry* **1999**, *38*, 2358–2366.
- (27) Koide, K.; Bunnage, M. E.; Gomez Paloma, L.; Kanter, J. R.; Taylor, S. S.; Brunton, L. L.; Nicolaou, K. C. Molecular design and biological activity of potent and selective protein kinase inhibitors related to balanol. *Chem. Biol.* **1995**, *2*, 601–608.
- (28) Gustafsson, A. B.; Brunton, L. L. Differential and selective inhibition of protein kinase A and protein kinase C in intact cells by balanol congeners. *Mol. Pharmacol.* **1999**, *56*, 377–382.
- (29) Lampe, J. W.; Biggers, C. K.; Defauw, J. M.; Foglesong, R. J.; Hall, S. E.; Heerding, J. M.; Hollinshead, S. P.; Hu, H.; Hughes, P. F.; Jagdmann, G. E., Jr.; Johnson, M. G.; Lai, Y. S.; Lowden, C. T.; Lynch, M. P.; Mendoza, J. S.; Murphy, M. M.; Wilson, J. W.; Ballas, L. M.; Carter, K.; Darges, J. W.; Davis, J. E.; Hubbard, F. R.; Stamper, M. L. Synthesis and protein kinase inhibitory activity of balanol analogues with modified benzophenone subunits. *J. Med. Chem.* **2002**, *45*, 2624–2643.
- (30) Jagdmann, G. E.; Defauw, J. M.; Lampe, J. W.; Darges, J. W.; Kalter, K. Potent and selective PKC inhibitory five-membered ring analogues of balanol with replacement of the carboxamide moiety. *Bioorg. Med. Chem. Lett.* **1996**, *6*, 1759–1764.
- (31) Setyawan, J.; Koide, K.; Diller, T. C.; Bunnage, M. E.; Taylor, S. S.; Nicolaou, K. C.; Brunton, L. L. Inhibition of protein kinases by balanol: specificity within the serine/threonine protein kinase subfamily. *Mol. Pharmacol.* **1999**, *56*, 370–376.
- (32) Hall, S. E.; Ballas, L. M.; Kulanthaivel, P.; Boros, C.; Jiang, J. B.; Jagdmann, G. E., Jr.; Lai, Y.-S.; Biggers, C. K.; Hu, H.; et al. Preparation of balanoids as protein kinase C inhibitors. PCT Int. Appl. (Nichols, Gina M.; Sphinx Pharmaceuticals Corporation). WO9420062, 1994; 559 pp.
- (33) Hu, H.; Jagdmann, G. E., Jr.; Mendoza, J. S. Preparation of substituted fused and bridged bicyclic compound protein kinase C inhibitors. PCT Int. Appl. (Lilly, Eli, and Co.). WO9530640, 1995; 84 pp.
- (34) Barbier, P.; Stadlwieser, J.; Taylor, S. Novel azepanes and their ring homologs for therapy and prophylaxis of protein kinase mediated diseases. PCT Int. Appl. (F. Hoffmann-La Roche AG) WO9702249, 1997; 43 pp.
- (35) Barbier, P.; Huber, I.; Schneider, F.; Stadlwieser, J.; Taylor, S. Preparation of 3-amino/hydroxy-4-[4-benzoylphenylcarboxylamino/oxy]azepine and homolog protein kinase inhibitors. Eur. Pat. Appl. (F. Hoffmann-La Roche AG) EP663393, 1995; 47 pp.
- (36) Breitenlechner, C.; Gassel, M.; Hidaka, H.; Kinzel, V.; Huber, R.; Engh, R. A.; Bossemeyer, D. Protein Kinase A in Complex with Rho-kinase Inhibitors Y-27632, Fasudil (HA-1077), and H-1152P. Structural Basis of Selectivity. *Structure* **2003**, *11*, 1595–1607.
- (37) Masjost, B.; Ballmer, P.; Borroni, E.; Zürcher, G.; Winkler, F. K.; Jakob-Roetne, R.; Diederich, F. Structure-based design, synthesis, and in vitro evaluation of bi-substrate inhibitors for catechol O-methyltransferase (COMT). *Chem. Eur. J.* **2000**, *6*, 971–982.
- (38) Lerner, C.; Ruf, A.; Gramlich, V.; Masjost, B.; Zürcher, G.; Jakob-Roetne, R.; Borroni, E.; Diederich, F. X-ray crystal structure of a bisubstrate inhibitor bound to the enzyme catechol-O-methyltransferase: a dramatic effect of inhibitor preorganization on binding affinity. *Angew. Chem., Int. Ed.* **2001**, *40*, 4040–4042.
- (39) Lerner, C.; Masjost, B.; Ruf, A.; Gramlich, V.; Jakob-Roetne, R.; Zürcher, G.; Borroni, E.; Diederich, F. Bisubstrate inhibitors for the enzyme catechol-O-methyltransferase (COMT): Influence of inhibitor preorganization and linker length between the two substrate moieties on binding affinity. *Org. Biomol. Chem.* **2003**, *1*, 42–49.
- (40) Masjost, B. Structure-based design, synthesis, and in vitro evaluation of bisubstrate inhibitors for catechol O-methyltransferase (COMT). Ph.D. Dissertation; Swiss Federal Institute of Technology Zurich: Zurich, 2000.
- (41) Bossemeyer, D.; Engh, R. A.; Kinzel, V.; Ponstingl, H.; Huber, R. Phosphotransferase and substrate binding mechanism of the cAMP-dependent protein kinase catalytic subunit from porcine heart as deduced from the 2.0 Å structure of the complex with Mn<sup>2+</sup> adenyllyl imidodiphosphate and inhibitor peptide PKI(5–24). *EMBO J.* **1993**, *12*, 849–859.
- (42) Engh, R. A.; Girod, A.; Kinzel, V.; Huber, R.; Bossemeyer, D. Crystal structures of catalytic subunit of cAMP-dependent protein kinase in complex with isoquinolinesulfonyl protein kinase inhibitors H7, H8, and H89. Structural implications for selectivity. *J. Biol. Chem.* **1996**, *271*, 26157–26164.
- (43) Prade, L.; Engh, R. A.; Girod, A.; Kinzel, V.; Huber, R.; Bossemeyer, D. Staurosporine-induced conformational changes of cAMP-dependent protein kinase catalytic subunit explain inhibitory potential. *Structure (London)* **1997**, *5*, 1627–1637.
- (44) Johnson, D. A.; Akamine, P.; Radzio-Andzelm, E.; Madhusudan; Taylor, S. S. Dynamics of cAMP-Dependent Protein Kinase. *Chem. Rev. (Washington, D. C.)* **2001**, *101*, 2243–2270.
- (45) Schneider, T. Kinetische und strukturelle Untersuchungen zur Funktion ausgewählter konservierter Aminosäurereste der katalytischen Untereinheit Ca der Proteinkinase A. Ph.D. Dissertation; Universität Bielefeld: Bielefeld, 2002.
- (46) Gerber, P. R.; Müller, K. MAB, a generally applicable molecular force field for structure modelling in medicinal chemistry. *J. Comput.-Aided Mol. Des.* **1995**, *9*, 251–268.
- (47) *Insight II user guide*; Molecular Simulations Inc.: San Diego.
- (48) Matzinger, P. K.; Scalone, M.; Zutter, U. Process and intermediates for preparing azepines. Eur. Pat. Appl. (F. Hoffmann-La Roche AG) EP802190, 1997; 18 pp.
- (49) Wolfe, J. P.; Buchwald, S. L. Room-temperature catalytic amination of aryl iodides. *J. Org. Chem.* **1997**, *62*, 6066–6068.
- (50) Cardona, M. L.; Fernandez, M. I.; Garcia, M. B.; Pedro, J. R. Synthesis of natural polyhydroxystilbenes. *Tetrahedron* **1986**, *42*, 2725–2730.
- (51) Mancuso, A. J.; Huang, S.-L.; Swern, D. Oxidation of long-chain and related alcohols to carbonyls by dimethyl sulfoxide “activated” by oxalyl chloride. *J. Org. Chem.* **1978**, *43*, 2480–2482.
- (52) Patel, B. A.; Kim, J.-I. I.; Bender, D. D.; Kao, L.-C.; Heck, R. F. Palladium-catalyzed three carbon chain extension reactions with acrolein acetals. A convenient synthesis of conjugated dienals. *J. Org. Chem.* **1981**, *46*, 1061–1067.
- (53) (a) Gassel, M.; Breitenlechner, C. B.; Rüger, P.; Jucknischke, U.; Schneider, T.; Huber, R.; Bossemeyer, D.; Engh, R. A. Mutants of Protein Kinase A that Mimic the ATP-binding Site of Protein Kinase B (AKT). *J. Mol. Biol.* **2003**, *329*, 1021–1034. (b) Wegge, T.; Breitenlechner, C.; Schäfer, W.; Thomas, U.; Künkele, K.-P.; Engh, R. A.; Masjost, B., unpublished results.
- (54) Kraulis, P. J. MOLSCRIPT: a program to produce both detailed and schematic plots of protein structures. *J. Appl. Crystallogr.* **1991**, *24*, 945–949.
- (55) Esnouf, R. M. An extensively modified version of MolScript that includes greatly enhanced coloring capabilities. *J. Mol. Graphics Modell.* **1997**, *15*, 132–134.
- (56) Esnouf, R. M. Further additions to MolScript version 1.4, including reading and contouring of electron-density maps. *Acta Crystallogr., Sect. D: Biol. Crystallogr.* **1999**, *D55*, 938–940.
- (57) Merritt, E. A.; Murphy, M. E. P. Raster3D version 2.0. A program for photorealistic molecular graphics. *Acta Crystallogr., Sect. D: Biol. Crystallogr.* **1994**, *D50*, 869–873.
- (58) Merritt, E. A.; Bacon, D. J. Raster3D: photorealistic molecular graphics. *Methods Enzymol.* **1997**, *277*, 505–524.

JM0310479